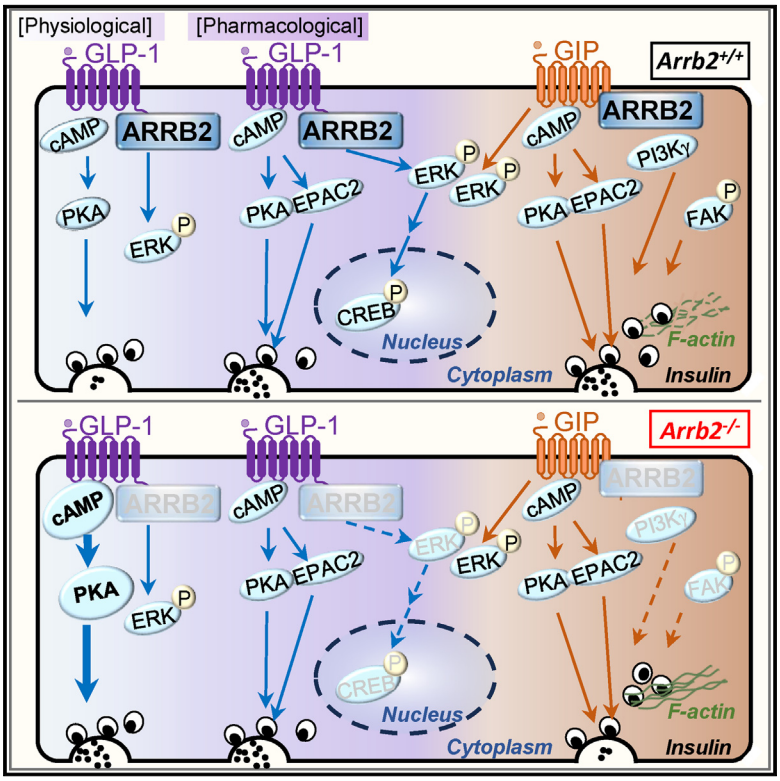
Cell Reports

Article

GLP-1 and GIP receptors signal through distinct β-arrestin 2-dependent pathways to regulate pancreatic β cell function

Graphical abstract



Highlights

- ARRB2 dampens insulin secretion at physiological doses of GLP-1
- ARRB2 is required for ERK1/2 and CREB activation at pharmacological doses of GLP-1
- GIP potentiation of glucose-induced insulin secretion requires ARRB2
- Diabetogenic conditions decrease ARRB2 levels in human islet cells

Authors

Nour Zaïmia, Joelle Obeid, Annie Varrault, ..., Safia Costes, Gyslaine Bertrand, Magalie A. Ravier

Correspondence

magalie.ravier@igf.cnrs.fr

In brief

Glucagon-like peptide 1 (GLP-1R) and glucose-dependent insulinotropic polypeptide (GIPR) receptors are involved in glucose homeostasis. Zaïmia et al. show that β-arrestin 2 (ARRB2) plays distinct roles in regulating GLP-1R/GIPR signaling. GIP-potentiated insulin secretion and ERK/CREB activation induced by pharmacological doses of GLP-1 require ARRB2. By contrast, ARRB2 dampens insulin secretion at physiological doses of GLP-1.

Zaïmia et al., 2023, Cell Reports *42*, 113326
November 28, 2023 © 2023 The Authors.
https://doi.org/10.1016/j.celrep.2023.113326

CellPress

Cell Reports

CellPress
OPEN ACCESS

Article

GLP-1 and GIP receptors signal through distinct β-arrestin 2-dependent pathways to regulate pancreatic β cell function

Nour Zaïmia,[1] Joelle Obeid,[1] Annie Varrault,[1] Julia Sabatier,[2] Christophe Broca,[2] Patrick Gilon,[3] Safia Costes,[1] Gyslaine Bertrand,[1] and Magalie A. Ravier[1,4,*]

[1]IGF, Université Montpellier, CNRS, INSERM, Montpellier, France
[2]LTCD, IRMB, CHU Montpellier, Montpellier, France
[3]Université Catholique de Louvain, Institut de Recherche Expérimental et Clinique, Pôle d'Endocrinologie, Diabète, et Nutrition, Brussels, Belgium
[4]Lead contact
*Correspondence: magalie.ravier@igf.cnrs.fr
https://doi.org/10.1016/j.celrep.2023.113326

SUMMARY

Glucagon-like peptide 1 (GLP-1R) and glucose-dependent insulinotropic polypeptide (GIPR) receptors are G-protein-coupled receptors involved in glucose homeostasis. Diabetogenic conditions decrease β-arrestin 2 (ARRB2) levels in human islets. In mouse β cells, ARRB2 dampens insulin secretion by partially uncoupling cyclic AMP (cAMP)/protein kinase A (PKA) signaling at physiological doses of GLP-1, whereas at pharmacological doses, the activation of extracellular signal-related kinase (ERK)/cAMP-responsive element-binding protein (CREB) requires ARRB2. In contrast, GIP-potentiated insulin secretion needs ARRB2 in mouse and human islets. The GIPR-ARRB2 axis is not involved in cAMP/PKA or ERK signaling but does mediate GIP-induced F-actin depolymerization. Finally, the dual GLP-1/GIP agonist tirzepatide does not require ARRB2 for the potentiation of insulin secretion. Thus, ARRB2 plays distinct roles in regulating GLP-1R and GIPR signaling, and we highlight (1) its role in the physiological context and the possible functional consequences of its decreased expression in pathological situations such as diabetes and (2) the importance of assessing the signaling pathways engaged by the agonists (biased/dual) for therapeutic purposes.

INTRODUCTION

Following meal ingestion, the gut-derived incretin hormones glucagon-like peptide 1 (GLP-1) and glucose-dependent insulinotropic polypeptide (GIP) are released by intestinal L and K cells, respectively. They are called "incretins" because, after oral ingestion of glucose, their intestinal release is responsible for the greater insulin secretion from pancreatic β cells compared with a similar intravenous glucose infusion, which does not release GLP-1 or GIP.[1] The incretin effect accounts for 50%–70% of post-prandial insulin secretion[1,2] and is therefore crucial to maintain glucose homeostasis. Moreover, both hormones have been reported to preserve the pancreatic β cell mass.[3,4] In type 2 diabetes (T2D), the incretin pathway is disturbed with a decreased insulinotropic response to GIP but not necessarily to GLP-1.[1] In consequence, current therapeutic strategies have focused on improving the durability, efficacy, and activity of GLP-1 using stable GLP-1 rather than GIP agonists. Nevertheless, it has been recently reconsidered to combine both incretins into a single molecule (GLP-1/GIP agonist) to benefit from the positive effects of each molecule on the pancreas and other target tissues to elicit additional glycemic and/or bodyweight controls.[1,5,6] Because of its therapeutic relevance, GLP-1 receptor (GLP-1R) has been studied more extensively than GIP receptor (GIPR), but the current availability of dual GLP-1/GIP agonists for therapeutic purposes has underscored the importance of further characterizing GIPR signaling along with GLP-1R signaling in native primary living cells.

GLP-1R and GIPR belong to the glucagon subfamily of class B G-protein-coupled receptors (GPCRs) and are preferentially positively coupled to $G\alpha_s$, yielding to cyclic AMP (cAMP) increase, protein kinase A (PKA), and exchange protein directly activated by cAMP 2 (EPAC2) activation.[3,7] β-Arrestin 2 (ARRB2), a scaffold protein that interacts with a wide range of GPCRs, is known to uncouple G-proteins from GPCRs but also to recruit additional signaling pathways, such as the extracellular signal-related kinase 1 and 2 (ERK1/2), phosphatidylinositol 3-kinase (PI3K), or focal adhesion kinase (FAK).[8,9] Interestingly, ARRB2 has been reported to play important roles in metabolic tissues to regulate glucose and energy homeostasis.[10] ARRB2 is recruited upon GLP-1 stimulation[11–13] to the GLP-1R[14] in recombinant clonal cell lines. ARRB2 downregulation has been reported by Jones et al.[13] to reduce GLP-1 induced insulin secretion from clonal β cell lines[13] and more recently from ARRB2 knockout mice (*Arrb2*$^{-/-}$),[15] with a minor role in GLP-1R internalization.[15,16] Nevertheless, we[17] and others[18] found similar insulin secretion in response to acute stimulation with pharmacological

This is an open access article under the CC BY-NC-ND license (http://creativecommons.org/licenses/by-nc-nd/4.0/).

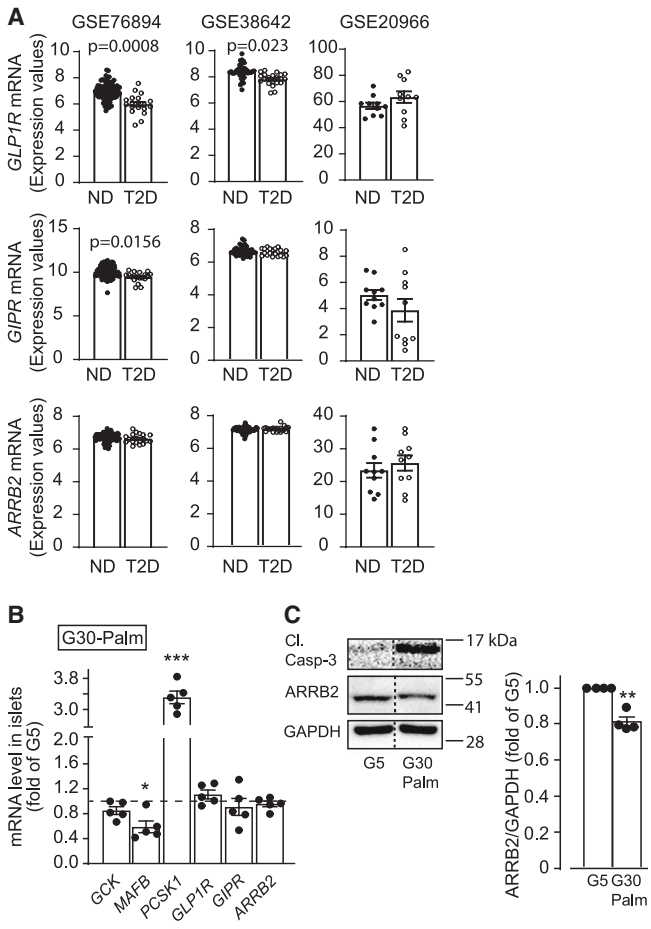


Figure 1. ARRB2 protein levels are decreased in human islets under diabetogenic conditions

(A) Analysis of islet transcriptomic expression of *GLP1R*, *GIPR*, and *ARRB2* in subjects with T2D compared with non-diabetic (ND) subjects based on three datasets (GEO: GSE76894 [https://tiger.bsc.es/; ND; n = 84 and T2D; n = 19], GSE38642 [ND; n = 42 and T2D or hyperglycemic; HbA1c ≥ 6%; n = 21], and GSE20966 [ND; n = 10 and T2D; n = 10]). Data are mean ± SEM; adjusted p values (multiple testing corrections).

(B and C) Isolated human islets were exposed for 72 h in control (5 mM glucose [G5]) or glucolipotoxic (30 mM glucose + 0.5 mM palmitate [G30-Palm]) conditions.

(B) Quantification of mRNA levels by qRT-PCR of *GCK* (glucokinase), *MAFB*, *PCSK1*, *GLP1R*, *GIPR*, and *ARRB2*, normalized to the geometric mean of the expression levels of two housekeeping genes (*ARP* and *L31*). The dotted line shows the normalized values for each gene in G5.

(C) Representative immunoblots of ARRB2, Cl. Casp-3 (cleaved caspase-3; showing apoptosis induced by G30-Palm), and GAPDH (used as a loading control) expression and quantitative analysis. Lanes of the immunoblots were run on the same gel but were non-continuous (as indicated). Data are mean ± SEM, n = 4–5 donors. *p < 0.05, **p < 0.01, ***p < 0.001 compared with G5. Student's t test.

concentrations of GLP-1 (20–100 nM) in *Arrb2*$^{+/+}$ and *Arrb2*$^{-/-}$ mouse β cells. On the other hand, while the role of ARRB2 in β cell protection by GLP-1 is not known, we and others have shown that whole-body *Arrb2*$^{-/-}$ mice display a reduced β cell mass and a limited β cell mass expansion under metabolic stress.[17,19]

The interaction of ARRB2 with the GIPR is less clear. Early studies have reported that GIP does induce ARRB2 recruitment to the GIPR in non-β cells,[12,20,21] while recent studies have found a crucial role of ARRB2 in trafficking and signaling of the GIPR.[16,22–24] Furthermore, only two studies with a limited number of experiments have evaluated the involvement of ARRB2 in the regulation of GIP-induced insulin secretion in clonal β cell line[16] and *Arrb2*$^{-/-}$ mice.[15]

To determine whether ARRB2 contributes to GLP-1R and GIPR signaling in primary β cells to regulate glucose homeostasis, we assessed the incretin effect in *Arrb2*$^{-/-}$ mice. In contrast to most studies that have investigated GLP-1R and GIPR downstream signaling in transfected cell lines overexpressing the proteins of interest (GLP-1R, GIPR, ARRBs, etc.),[11,15,16] we studied downstream signaling of GLP-1R and GIPR in native primary β cells from *Arrb2*$^{-/-}$ mice. Because 1–10 pM GLP-1 has been reported to be as effective as 1 nM GLP-1 in modulating electrical activity[25,26] and insulin secretion,[25,26] we evaluated the impact of physiological (<100 pM) and pharmacological (≥100 pM–10 nM) concentrations of GLP-1, the latter being measured after Roux-en-Y gastric bypass surgery[27] and in T2D patients treated with GLP-1R agonists.[28,29] Here we report a distinct role of ARRB2 in GLP-1R and GIPR signaling in primary β cells and therefore a specificity of action for two GPCRs belonging to the class B glucagon subfamily. ARRB2 contributes to a partial uncoupling of cAMP/PKA signaling in the physiological range of GLP-1 and, consequently, reduced insulin secretion. On the other hand, ARRB2 is also required for the recruitment of ERK1/2 and the activation of the transcription factor cAMP-responsive element-binding protein (CREB) induced by pharmacological doses of GLP-1. In contrast, ARRB2 plays a crucial role in GIP potentiation of insulin secretion independently from the canonical cAMP signaling (PKA and EPAC2) and the ERK1/2 pathway but through F-actin depolymerization. PI3Kγ recruitment and/or FAK activation are likely involved in that process. Our study emphasizes the physiological role of ARRB2 and the possible functional consequences of its decreased expression in pathological situations. It also highlights the importance of evaluating the signaling pathways engaged by different agonists (biased or dual agonists) for future therapeutic purposes of targeting GLP-1R and/or GIPR, taking into account the specific and non-redundant roles of ARRB2.

RESULTS

Decreased ARRB2 protein levels in human islets under diabetogenic conditions

Because subjects with T2D have an impaired insulinotropic response to GIP but retain a response to GLP-1,[1] islet transcriptome data for GLP-1R and GIPR expression in T2D islets were retrieved from three available datasets (TIGER resource [https://tiger.bsc.es/][30] and GEO: GSE76894,[31] GSE38642,[32] and GSE20966[33]). The analysis showed that *GLP1R* mRNA levels are slightly decreased in two of three datasets compared with non-diabetic controls (Figure 1A). *GIPR* mRNA levels are also only slightly decreased in one of three datasets. In broad terms, the expression of GLP-1R and GIPR, at the mRNA level, does not seem to be consistently altered in T2D. Additionally, the *ARRB2* mRNA levels in T2D samples remained unchanged in all datasets (Figure 1A). In human islets treated under glucolipotoxic

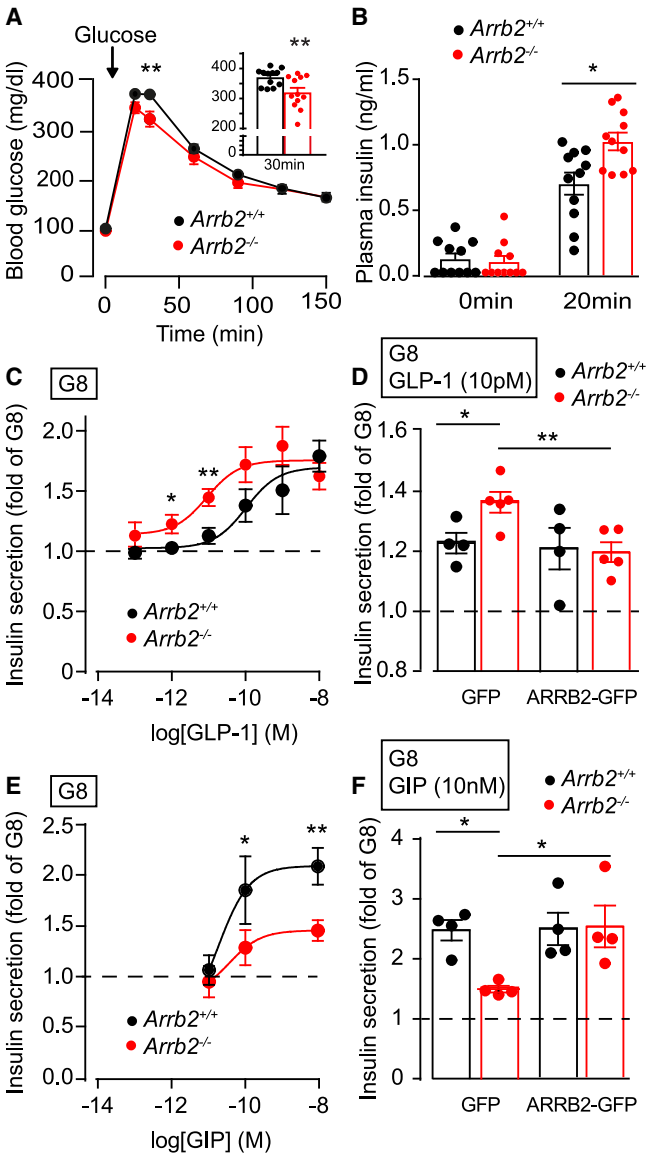


Figure 2. *Arrb2*$^{-/-}$ mice have an enhanced incretin effect that is associated with increased insulin secretion in response to physiological concentrations of GLP-1 despite a decreased insulin secretion in response to GIP

(A) Blood glucose levels before and after oral glucose administration (oral glucose tolerance test [OGTT]; 1.5 g/kg body weight). The inset shows blood glucose values for each mouse 30 min after the oral glucose load.

(B) Plasma insulin levels before (0) and 20 min after glucose load during the OGTT.

(C) Insulin secretion from isolated mouse islets in response to GLP-1 in the presence of 8 mM glucose (G8).

(D) Insulin secretion in response to 10 pM GLP-1 from mouse islets expressing either GFP (control) or ARRB2-GFP.

(E) Insulin secretion from isolated islets in response to GIP in the presence of G8.

(F) Insulin secretion in response to 10 nM GIP in islets expressing either GFP (control) or ARRB2-GFP.

Data are means ± SEM for 11–12 (A and B), 6–8 (C), 4–5 (D), 6 (E), and 4 (F) mice. *p < 0.05, **p < 0.01. One-way ANOVA (C and E) or two-way ANOVA (A, B, D, and F) followed by Sidak's post test.

conditions (30 mM glucose + 0.5 mM palmitate [G30-Palm]), mimicking the diabetic environment, *GLP1R*, *GIPR*, and *ARRB2* mRNA expression levels were not altered (Figure 1B), while decreased *MAFB* and increased *PCSK1* mRNA levels were observed (Figure 1B), as expected.[34] However, despite similar mRNA levels, ARRB2 protein expression was significantly decreased by 20% under glucolipotoxic conditions (Figure 1C). This is consistent with previous reports showing that ARRB2 protein expression is reduced in metabolic tissues (such as adipose tissue, liver, and muscle),[35] in islets[36] from diabetic[35,36] mice or mice maintained on a high-fat diet,[35,36] and in liver samples from human subjects with T2D.[35] All of these results indicate that ARRB2 protein expression is broadly decreased in the context of metabolic disease.

Improved incretin effect in *Arrb2*$^{-/-}$ mouse and higher insulin secretion upon physiological concentrations of GLP-1 from *Arrb2*$^{-/-}$ pancreatic islets

To investigate the impact of the absence of ARRB2, whole-body *Arrb2*$^{-/-}$ mice were used. We[17] and others[35] have previously reported an impairment in glucose tolerance and altered insulin secretion in *Arrb2*$^{-/-}$ mice when glucose was injected intraperitoneally and a similar sensitivity to insulin[15,17] in *Arrb2*$^{+/+}$ and *Arrb2*$^{-/-}$ mice. Here we further report that, in contrast to intraperitoneally injected glucose, *Arrb2*$^{-/-}$ mice displayed better glucose tolerance 30 min after oral administration of the sugar compared with *Arrb2*$^{+/+}$ mice (Figure 2A and inset). This was concomitant with higher plasma insulin levels (Figure 2B). By contrast, plasma levels of active GIP (Figure S1A) and glucagon (Figure S1B) were similar in *Arrb2*$^{+/+}$ and *Arrb2*$^{-/-}$ mice, whereas active GLP-1 levels could not be measured. These results suggest that *Arrb2*$^{-/-}$ mice have a slightly enhanced incretin effect. To determine whether the increased plasma insulin concentration during the oral glucose tolerance test in *Arrb2*$^{-/-}$ mice was related to an improvement of the GLP-1R and/or GIPR signaling in pancreatic β cells, pancreatic islets were isolated from *Arrb2*$^{+/+}$ and *Arrb2*$^{-/-}$ mice. Insulin secretion was augmented 6-fold in response to 8 mM glucose compared with a non-stimulatory glucose concentration (G3) and similarly in *Arrb2*$^{+/+}$ and *Arrb2*$^{-/-}$ islets (Figure S2A). By contrast, insulin secretion was greater in response to physiological circulating concentrations of GLP-1 (1–10 pM) (Figures 2C and S2E) in *Arrb2*$^{-/-}$ compared with *Arrb2*$^{+/+}$ islets, while no differences were observed upon pharmacological concentrations (≥100 pM–10 nM) (Figures 2C and S2E). In *Arrb2*$^{+/+}$ β cells, overexpressing ARRB2 (ARRB2-GFP) affected neither islet insulin content (Figure S2B) nor insulin secretion in response to 8 mM glucose or in response to 10 pM GLP-1 (Figure S2C). In contrast, reintroducing ARRB2 (ARRB2-GFP) into *Arrb2*$^{-/-}$ islet β cells restored insulin secretion to levels similar to those in *Arrb2*$^{+/+}$ islets in response to 10 pM GLP-1 (Figures 2D and S2C), showing that this effect is due to ARRB2. GIP was only effective from 100 pM (Figure 2E), which is not surprising because circulating concentrations of GIP[37,38] are considered to be slightly higher than those of GLP-1,[37,38] and it has already been reported that β cells respond to doses of GLP-1 lower than GIP.[39] Unexpectedly, in contrast to GLP-1, GIP-potentiated insulin secretion was blunted in *Arrb2*$^{-/-}$ islets (Figures 2E and S2E), while the dual

GLP1R/GIPR agonist tirzepatide (TZP)[6,40] induced similar insulin secretion from *Arrb2*$^{+/+}$ and *Arrb2*$^{-/-}$ islets (Figure S2E).

Again, reintroducing ARRB2 (ARRB2-GFP) in *Arrb2*$^{-/-}$ islets restored insulin secretion (Figures 2F and S2D). Of note, the experiments were performed under 8 mM glucose, which is close to the fed blood glucose concentration in *Arrb2*$^{+/+}$ mice (8.39 ± 0.67 mM, n = 10), but similar results were observed with 15 mM glucose (Figure S2F), a concentration that is reached during the oral glucose tolerance test. Although not significant, the response to 10 pM GLP-1 in *Arrb2*$^{-/-}$ islets showed a tendency to be increased (Figure S2F). Overall, our results indicate that the better oral glucose tolerance of *Arrb2*$^{-/-}$ mice is associated with increased insulin secretion *in vivo*, which might be partly caused by an improved insulinotropic response to GLP-1 from pancreatic β cells.

Increased cAMP production, PKA activation, and $[Ca^{2+}]_c$ changes upon physiological concentrations of GLP-1 in *Arrb2*$^{-/-}$ mouse β cells

Next, we investigated the contribution of ARRB2 to GLP-1R signaling by measuring cAMP production and the resulting activation of PKA and EPAC2 recruitment underneath the plasma membrane in living mouse β cells. Physiological concentrations of GLP-1 (<100 pM) induced significantly higher cAMP production (Figures 3A and 3D) and PKA activity (Figures 3B, 3C, 3E, and 3F) in *Arrb2*$^{-/-}$ compared with *Arrb2*$^{+/+}$ β cells, while no differences were observed upon pharmacological (≥100 pM) concentrations (Figures 3A, 3C, 3D, 3F, S3A, and S3B). By contrast, EPAC2 was not recruited underneath the plasma membrane in response to 10 pM GLP-1 (Figures 3G and 3I), while 10 nM GLP-1 recruited EPAC2 similarly in *Arrb2*$^{-/-}$ and in *Arrb2*$^{+/+}$ β cells (Figures 3H and 3I).

GLP-1 is known to exert a depolarizing effect on the electrical activity, partly through the closure of K_{ATP} channels but also through an increase of a background inward Na^+ current carried by TRPM4 and TRPM5 channels.[25] Upon 10 pM GLP-1, we observed no significant impact on $[Ca^{2+}]_c$ oscillation frequencies (Figures 4A, 4B, 4D, and 4E) and mean levels (Figure 4F) in *Arrb2*$^{+/+}$ β cells compared with 8 mM glucose alone, while $[Ca^{2+}]_c$ oscillation frequencies (Figures 4C–4E) and mean $[Ca^{2+}]_c$ levels (Figure 4F) were significantly increased in *Arrb2*$^{-/-}$ β cells. By contrast, pharmacological concentrations of GLP-1 induced similar $[Ca^{2+}]_c$ oscillation frequency changes and mean levels in *Arrb2*$^{+/+}$ and *Arrb2*$^{-/-}$ β cells (Figures 4E and 4F).

Taken together, these results show that the higher insulin release induced by physiological concentrations of GLP-1 in the absence of ARRB2 is associated with a greater cAMP production, PKA activity, and $[Ca^{2+}]_c$ changes without any contribution of EPAC2 recruitment.

Similar diacylglycerol levels upon physiological concentrations of GLP-1 in *Arrb2*$^{-/-}$ and *Arrb2*$^{+/+}$ mouse β cells

Physiological concentrations of GLP-1 have been reported to involve Gαq signaling, resulting in increased diacylglycerol (DAG) levels and protein kinase C (PKC) activation.[25] The addition of 10 pM GLP-1 increased DAG levels ($p < 0.05$) similarly in *Arrb2*$^{+/+}$ and *Arrb2*$^{-/-}$ β cells (Figure S4A), but GLP-1 was less potent than the muscarinic agonist acetylcholine (Figure S4A). Surprisingly, in contrast to acetylcholine, the increase in DAG levels upon GLP-1 stimulation was neither followed by Ca^{2+} release from the endoplasmic reticulum ($[Ca^{2+}]_{ER}$) (Figures S4B and S4C), which could reflect inositol 1,4,5 triphosphate production, nor by the recruitment of PKCβII to the plasma membrane (Figures S4D and S4E). Thus, ARRB2 is not involved in the production of DAG in response to GLP-1, and GLP-1 does not trigger PKCβII activation.

ARRB2 is required for full activation of ERK1/2 and CREB upon pharmacological GLP-1 stimulation

ARRB2 is known as a scaffold protein that recruits additional signaling pathways to the activated GPCR, such as ERK1/2. ERK1/2 are activated by GLP-1,[11] but the involvement of ARRB2 in activating ERK1/2 upon GLP-1 stimulation[11] is still unclear in mouse β cells. We observed that ERK1/2 activation, assessed by immunocytochemistry,[41] was significantly increased by physiological concentration of GLP-1 (10 pM; 1.90 ± 0.06-fold of 8 mM glucose (G8) in *Arrb2*$^{+/+}$ β-cells; $p < 0.05$ compared with G8) but to the same extent in *Arrb2*$^{+/+}$ and *Arrb2*$^{-/-}$ β cells (1.90 ± 0.06 vs. 1.46 ± 0.20-fold of G8; respectively; not significant) (Figures 5A and 5B). By contrast, ERK1/2 activation was significantly reduced in *Arrb2*$^{-/-}$ β cells in response to pharmacological concentrations of GLP-1 (1–10 nM; Figures 5A and 5B). This was restored/reinforced when ARRB2 (ARRB2-GFP) was reintroduced in *Arrb2*$^{-/-}$ β cells (Figures 5C and 5D). Cytosolic ERK1/2 activity, evaluated in living β cells using the fluorescence resonance energy transfer (FRET)-based sensor cytoEKAR,[41] was less sustained upon physiological concentrations of GLP-1 versus sustained upon pharmacological concentrations (Figures 5E and 5F). Consistent with immunocytochemistry experiments, ERK1/2 activity was only reduced in response to pharmacological concentrations of GLP-1 in *Arrb2*$^{-/-}$ compared with *Arrb2*$^{+/+}$ β cells (Figures 5E and 5F). Overall, these results indicate that ARRB2 is required for full activity of ERK1/2 only in response to pharmacological concentrations of GLP-1.

CREB is mainly phosphorylated at Ser133 by PKA but also by MSK1 and p90RSK, two direct targets of ERK1/2.[41] Only pharmacological doses (1–10 nM) of GLP-1 increased nuclear CREB phosphorylation in *Arrb2*$^{+/+}$ β cells (Figures 5G and 5H), and this effect was abrogated in *Arrb2*$^{-/-}$ β cells (Figures 5G and 5H). These results indicate that ARRB2 is essential for full activation of ERK1/2 and CREB by pharmacological concentrations of GLP-1.

ARRB2 is required for proper insulin secretion in response to GIP through actin depolymerization, PI3Kγ, and FAK activation

Although GLP-1 and GIP act through $G\alpha_s$-coupled class B GPCRs, the deletion of *Arrb2* exerts opposite effects on insulin secretion. Indeed, ARRB2 is required for GIP potentiation of insulin secretion in mouse islets (Figures 2E, 2F, and S2D–S2F). To determine whether ARRB2 is also involved in humans, ARRB2 expression was downregulated in human islets using adenovirally transduced short hairpin RNA (shRNA) (Figures 6A and 6B). A decrease in ARRB2 expression by 20% (Figure 6B) significantly reduced insulin secretion from human islets in response to GIP but not to GLP-1 (Figure 6C). Moreover, although not

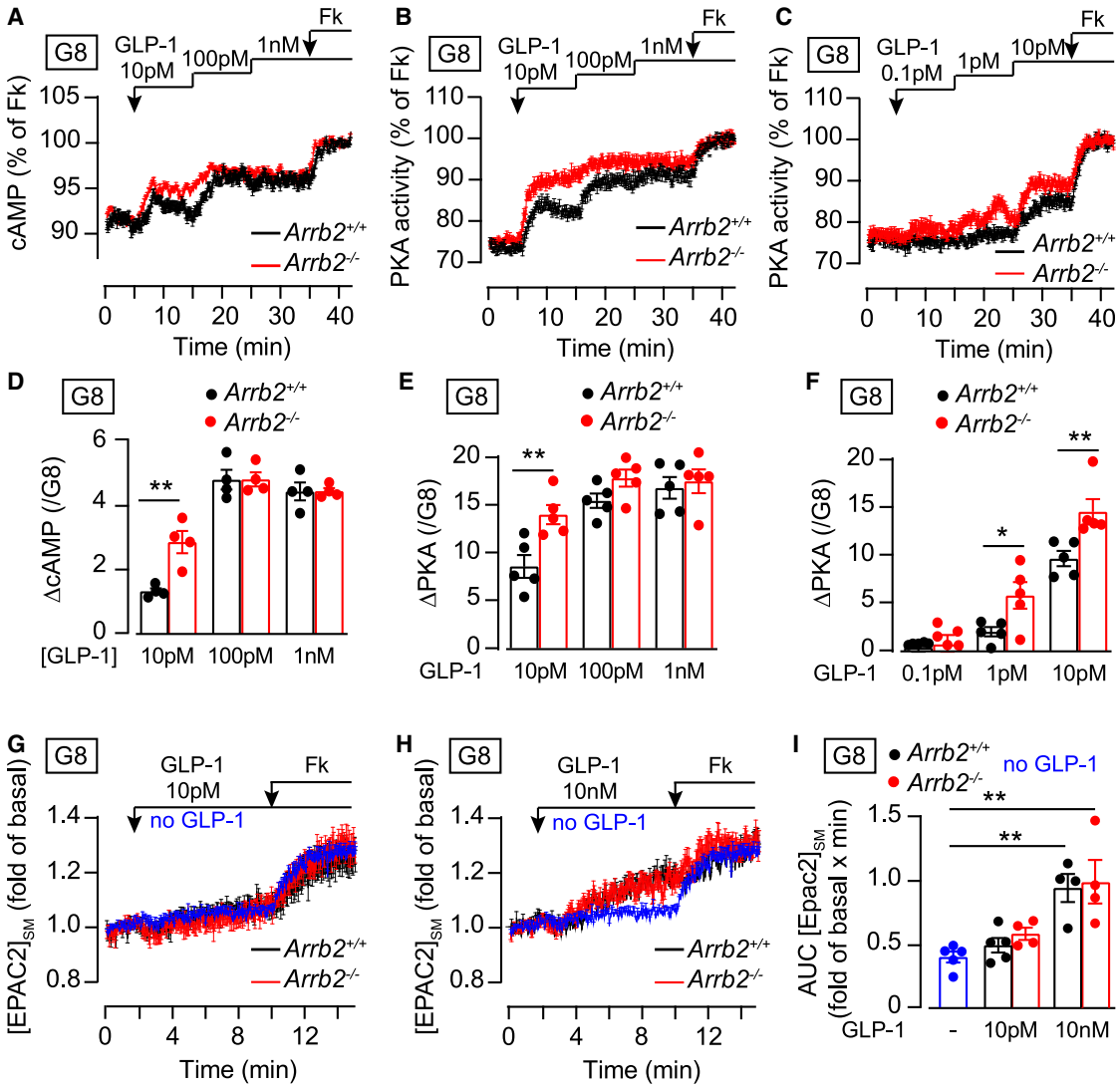


Figure 3. cAMP production and PKA activation, but not EPAC2 recruitment, are further increased in response to physiological concentrations of GLP-1 in *Arrb2*$^{-/-}$ mouse β cells

(A–I) GLP-1 concentrations were increased in the presence of G8, as indicated. Traces were normalized to forskolin (Fk; 1 μM) which directly stimulates adenylate cyclase and maximally increases cAMP production. Please note that cAMP production was only measured from 10 pM (and not at 0.1–1 pM) GLP-1 because of the small ratio variations measured with the EPAC2B-camps probe (low sensitivity) compared with those measured for PKA activity with the AKAR3 probe. Shown are measurements of cAMP production (A and D), PKA activity (B, C, E, and F) and EPAC2 recruitment beneath the plasma membrane by total internal reflection fluorescence (TIRF) microscopy in dispersed islet cells (G–I). The blue line is without the addition of GLP-1; *Arrb2*$^{+/+}$. Shown in (D)–(F) is quantifications of cAMP production and PKA activity from (A)–(C). Data are means ± SEM for 4 mice (20 cells, A); 5 mice (44–55 cells, B and C), and 4–5 mice (17–25 cells, G and H). *p < 0.05, **p < 0.01 compared with *Arrb2*$^{+/+}$. One-way ANOVA followed by Sidak's post test.

significant (p = 0.1008), insulin secretion in response to the dual GLP-1R/GIPR agonist TZP was still diminished in 3 of 4 batches of human islets when ARRB2 expression was reduced (Figure 6C).

To further investigate the molecular mechanisms involved in the alteration of insulin secretion in response to GIP, islet cells from *Arrb2*$^{-/-}$ mice were used. Unexpectedly, upon GIP stimulation, cAMP production (Figure 6D), PKA activity (Figures 6E, S5E), EPAC2 recruitment underneath the plasma membrane (Figure 6F), Ca^{2+} signaling (Figures S5A–S5D, S5F, and S5G), and ERK1/2 activity (Figure 6G) were similar in *Arrb2*$^{+/+}$ and *Arrb2*$^{-/-}$ mouse β cells. Additionally, GIP did not trigger PKCβII recruitment underneath the plasma membrane (Figure S5H). In summary, the reduction of GIP-potentiated insulin secretion in the absence of ARRB2 is not the result of an impairment in cAMP production, recruitment of PKA, EPAC2, or ERK1/2 or changes in $[Ca^{2+}]$.

In parallel to the canonical cAMP pathway, PI3Kγ signaling has been reported to be required for GIP- but not GLP-1-dependent actin depolymerization and insulin secretion.[42] We observed similar F-actin depolymerization, attested by a lower

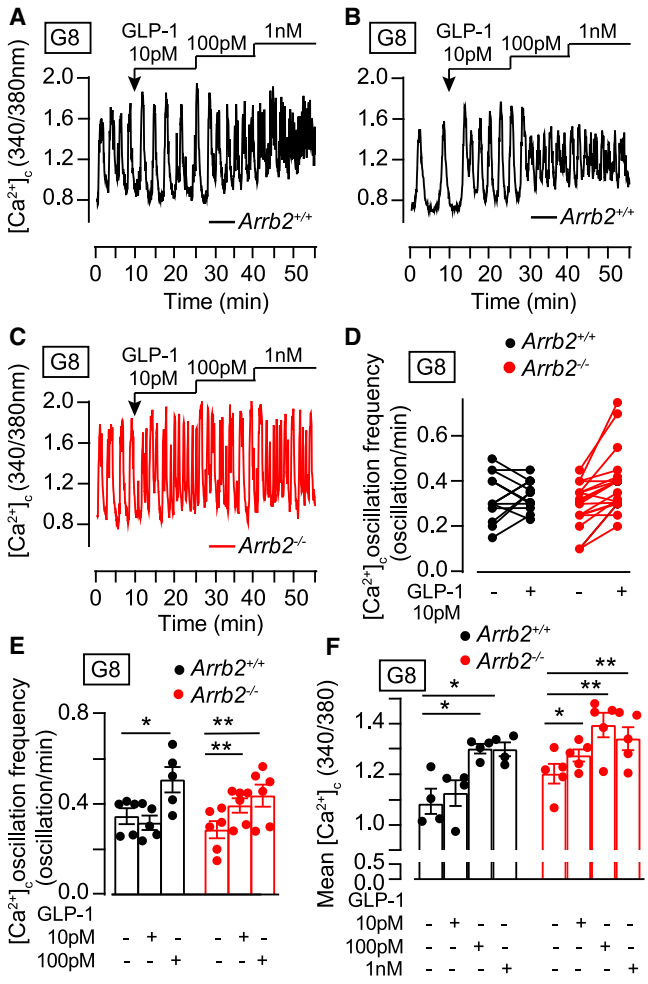


Figure 4. $[Ca^{2+}]_c$ frequencies and mean levels are increased in response to physiological concentrations of GLP-1 in *Arrb2*$^{-/-}$ β cells

(A–C) GLP-1 concentrations were increased in the presence of G8, as indicated. Representative individual $[Ca^{2+}]_c$ traces were measured in *Arrb2*$^{+/+}$ (A and B, two independent experiments) and *Arrb2*$^{-/-}$ (C) dispersed islet cells.

(D) $[Ca^{2+}]_c$ oscillation frequencies in the absence and presence of 10 pM GLP-1 (from A–C).

(E and F) Mean $[Ca^{2+}]_c$ oscillation frequencies (E) and levels (F) quantified in the absence (0–10 min) or presence of GLP-1 (15–25 min, 30–40 min, and 45–55 min, respectively).

Note that $[Ca^{2+}]_c$ oscillation frequencies were not quantified at 1 nM GLP-1 because most of the clusters displayed a mixed pattern with fast oscillations superimposed on slow oscillations (A) or a sustained elevated level (data not shown). Data are representative traces (A–C) and means ± SEM (D–F) for 4–6 mice (15–20 clusters of cells). *p < 0.05, **p < 0.01. One-way ANOVA for repeated measures followed by Tukey's post test.

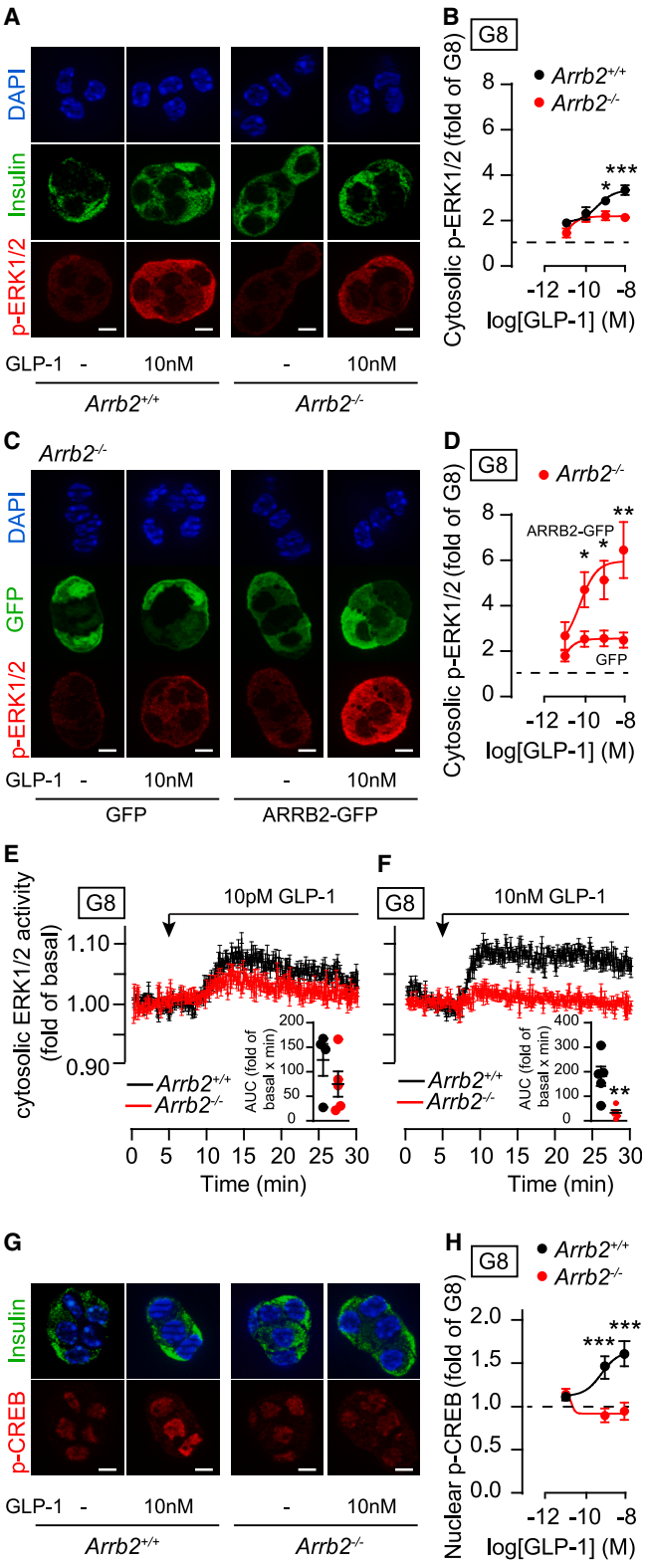
peak fluorescence intensity at the plasma membrane, upon 10 pM and 10 nM GLP-1 in *Arrb2*$^{+/+}$ and *Arrb2*$^{-/-}$ β cells (Figures 7A and 7B). By contrast, a significant reduction of F-actin depolymerization upon 10 nM GIP was observed in *Arrb2*$^{-/-}$ compared with *Arrb2*$^{+/+}$ β cells (Figures 7A and 7B). As reported previously,[42] a PI3Kγ inhibitor (AS604850, 1 μM) reduced F-actin depolymerization upon GIP but not GLP-1 stimulation in *Arrb2*$^{+/+}$ β cells (Figure 7C). No supplementary effects were observed upon PI3Kγ inhibition in *Arrb2*$^{-/-}$ β cells (Figure 7C), indicating that ARRB2 and PI3Kγ likely share a common signaling pathway leading to actin depolymerization upon GIP stimulation. Furthermore, it has been reported that FAK is required for remodeling of the actin cytoskeleton for proper insulin secretion.[43] Additionally, FAK has been shown to form a complex with ARRB2 to be recruited to GPCRs, allowing its subsequent activation by G-proteins.[8] GLP-1 and GIP induced FAK activation in *Arrb2*$^{+/+}$ β cells (Figures 7E and 7F), which was reduced in *Arrb2*$^{-/-}$ β cells upon GIP but not GLP-1 stimulation (Figures 7E and 7F). The phosphorylation of Paxillin, a FAK-interacting protein localized to focal adhesions that mediates the reorganization of the cytoskeleton, was also increased in response to GLP-1 and GIP in *Arrb2*$^{+/+}$ β cells (Figure S6). Similar to FAK, Paxillin activation was reduced in *Arrb2*$^{-/-}$ β cells upon GIP but not GLP-1 stimulation (Figure S6). Finally, inhibiting ARRB/β2-adaptin interaction with barbadin[8] abrogated FAK and Paxillin activation in *Arrb2*$^{+/+}$ β cells (Figures 7F, S6) and significantly decreased F-actin depolymerization upon GIP but not GLP-1 stimulation (Figure 7D), indicating the involvement of the ARRB/FAK/Paxillin complex in the depolymerization of F-actin upon GIP stimulation. In summary, ARRB2 is essential for F-actin depolymerization upon GIP but not GLP-1 stimulation, and the identified mechanisms involved PI3Kγ signaling and FAK/Paxillin activation.

DISCUSSION

ARRB2 has been reported to play an important role in the regulation of glucose and energy homeostasis in metabolic tissues using mice in which the *Arrb2* gene has been inactivated in the whole organism[17,35] or conditionally in adipocytes,[44] hepatocytes,[45] and β cells.[15,18] This latter strategy is necessary to discriminate the role of ARRB2 in each tissue because of the difficulty of interpreting the metabolic phenotype *in vivo* or to dissect the potential role of ARRB2 in β cells *in vitro* in a mixed organ such as pancreatic islets. Nevertheless, one could also object that ARRB2 expression is broadly decreased in the context of metabolic diseases,[18,35,45] and therefore whole-body inactivation of the *Arrb2* gene might also better reflect physiopathological situations. In this study, we used whole-body inactivation of the *Arrb2* gene and assessed its impact on pancreatic β cell physiology in response to GLP-1 and GIP.

We report that ARRB2 plays a distinct role in regulating GLP-1R and GIPR signaling in β cells and thus highlight (1) its specificity of action for two GPCRs belonging to the class B GPCR positively coupled to cAMP production, (2) its importance in the physiological context, and (3) its potential relevance in the pathological context that should be considered for therapeutics.

Arrb2$^{-/-}$ mice display an improved incretin effect compared with *Arrb2*$^{+/+}$ mice. This is likely attributable to increased GLP-1R signaling, evidenced by enhanced cAMP/PKA/insulin secretion at physiological doses of GLP-1, whereas insulin secretion in response to GIP is reduced in *Arrb2*$^{-/-}$ β cells. These results were unexpected because GIP is thought to be responsible for the majority of the incretin effect,[1] but the improvement of GLP-1R signaling very likely compensated for this defect to a



greater extent. ARRB2 partially uncouples the GLP-1R for cAMP production, PKA activation, $[Ca^{2+}]_c$ changes, and finally insulin secretion upon physiologically relevant concentrations (<100 pM) but not upon pharmacological concentrations (≥100 pM) of GLP-1, as already reported for the latter.[17,18] By contrast, a recent study has reported decreased cAMP production/insulin secretion in response to pharmacological doses of a GLP-1 agonist (exendin 4) in *Arrb2*$^{-/-}$ mouse β cells,[15] while the impact of physiological doses was not investigated. The authors have reported that this effect was potentially mediated by compensatory β-arrestin 1 binding in the absence of ARRB2. Whether this effect is specific to their mouse colony needs to be determined because this effect was not observed in two other independent colonies.[17,18] Additionally, we observed that, with pharmacological concentrations of GLP-1, the activation of ERK1/2 and CREB requires ARRB2, which is in agreement with a recent report for a clonal β cell line.[15] The differential cellular output related to different concentrations of agonists has already been reported for other GPCRs[46] and for GLP-1 in mouse β cells with low versus high concentrations activating PKC and PKA, respectively.[25] It has also been reported in human adipocytes, where picomolar GLP-1 promoted lipogenesis, whereas nanomolar GLP-1 induced lipolysis.[47] Nevertheless, the contribution of ARRB2 was not addressed in this context. The plasma concentration of biologically active GLP-1 is in the picomolar range and does not increase beyond 10–60 pM even after meal ingestion,[27,37,38] or in T2D patients treated with a dipeptidylpeptidase IV inhibitor.[38] By contrast, pharmacological doses (>100 pM) could be measured after Roux-en-Y gastric bypass surgery[27] and in T2D patients treated with GLP-1R agonists.[28,29]

Because decreased expression of ARRB2 has been observed in diabetogenic situations (our study and previous studies[18,36]), the differential effects of physiological versus pharmacological doses of GLP-1 may therefore have functional consequences depending on the metabolic state. Additionally, despite clear cAMP production and PKA activation with physiological concentrations of GLP-1, EPAC2 is recruited beneath the plasma membrane only upon pharmacological activation of GLP-1R, which is consistent with the report that EPAC2 has a lower affinity for cAMP than PKA. This indicates that PKA, rather than EPAC2, is involved in GLP-1-induced insulin secretion after a meal.

Figure 5. ARRB2 is required for GLP-1-induced full activation and activity of ERK1/2 and CREB

(A–D) Representative immunocytochemistry images of the phosphorylated form of ERK1/2 (p-ERK1/2) representing ERK1/2 activation in dispersed islet cells (A and C) and quantitative analysis (B and D). Cells were in the presence of G8 and in the absence or presence of GLP-1. Panels showing green fluorescnce intensity are insulin immunoreactivity (A), GFP-expressing (C), or ARRB2-GFP-expressing (C) cells, as indicated. Only cells expressing insulin, GFP, or ARRB2-GFP were analyzed. For clarity, only images without GLP-1 and with 10 nM GLP-1 are shown.

(E and F) Measurements in dispersed islet cells of ERK1/2 activity, using the EKAR probe, in response to 10 pM (E) or 10 nM (F) GLP-1 in the presence of G8. Insets illustrate the AUC (5–30 min) for each individual mouse, one dot being the average of 7–13 cells from the same mouse.

(G and H) Representative immunocytochemistry images of the phosphorylated form of CREB (p-CREB) (G) in dispersed islet cells and quantitative analysis (H). Only cells expressing insulin were analyzed.

Scale bars, 5 μm. Data are mean ± SEM, n = 4 mice (B and D), n = 5 mice (E and F), and n = 6 mice (G and H). *p < 0.05, **p < 0.01, ***p < 0.001 compared with *Arrb2*$^{+/+}$ (B, F, and H) or *Arrb2*$^{-/-}$ expressing GFP (D). Student's t test (F) or one-way ANOVA followed by Sidak's post test (B, D, and H).

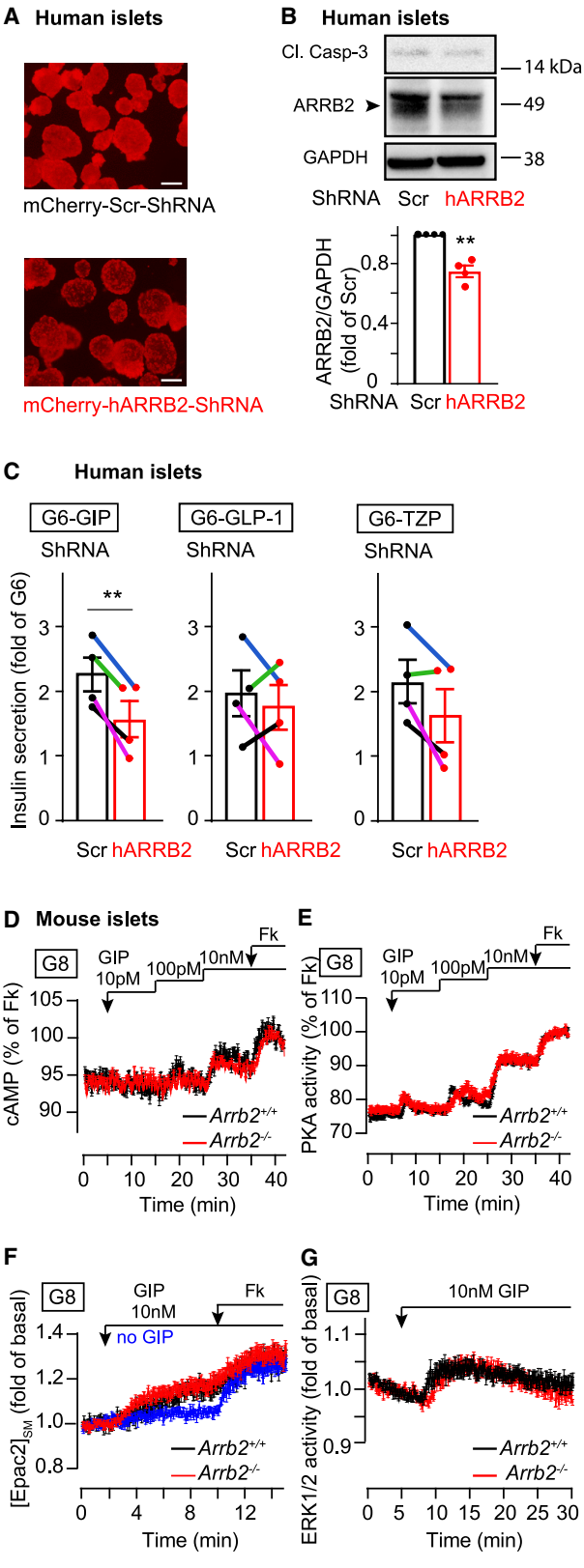


Figure 6. In response to GIP, ARRB2 is required for insulin secretion but not for cAMP and ERK1/2 signaling pathways

(A–C) Human islets were adenovirally transduced with mCherry-Scr-shRNA (scramble) and mCherry-hARRB2-shRNA.

(A) Representative images of mCherry expression in human islets, showing the efficacy of infection with each adenovirus. Scale bars, 100 μm.

(B) Representative immunoblots of ARRB2, Cl. Casp-3 (showing apoptosis), and GAPDH (used as a loading control) expression and quantitative analysis.

(C) Insulin secretion from human islets in response to GIP (10 nM), GLP-1 (10 nM), or TZP (10 nM) as indicated, in the presence of 6 mM glucose (G6). Data are mean ± SEM, n = 4 donors identified by colored lines. **p < 0.01 compared with Scr. Paired Student's t test.

(D–G) GIP was added in the presence of G8, and measurements were performed in dispersed mouse islet cells. Traces have been normalized to Fk (1 μM), which directly stimulates the adenylate cyclase and maximally increases cAMP production. Shown are measurements of cAMP production (D), PKA activation (E), EPAC2 recruitment beneath the plasma membrane by TIRF microscopy (F; the blue line is without GIP), and ERK1/2 activity (G) in dispersed islet cells.

Data are means ± SEM for 4 mice (22 cells, D), 5–6 mice (50 cells, E), and 4 mice (25–30 cells, F and G).

We did not explore the molecular mechanisms involved in the partial uncoupling of GLP-1R by ARRB2 for low concentrations of GLP-1, but two types of conformations of GPCR/ARRBs complexes have been reported for class B GPCRs with either ARRBs primarily coupled to the C-terminal tail of the receptor (tail conformation) or ARRBs further engaged within the receptor transmembrane core (core conformation).[48] In contrast to the core conformation that uncouples the GPCR from the G protein, the tail conformation allows G protein signaling in addition to the recruitment of ARRBs in internalized GPCRs.[48] Whether a similar mechanism applies to GLP-1R depending on the concentration of GLP-1 is an open question, but few studies have shown a beneficial effect of GLP-1R internalization that was associated with a maximal amount of cAMP production,[11,12,49] while others have shown a greater insulin release when GLP-1R was retained at the plasma membrane.[13] The biological reason for this partial uncoupling at physiological GLP-1 concentrations is unclear, but it could be argued that this desensitization is a protective mechanism for β cells to not release insulin when the insulin demand is low. Indeed, GLP-1R may be constitutively active,[50] and the presence of GLP-1 in surrounding α cells and the possibility of GLP-1R activation by glucagon may also be responsible, at least in part, for GLP-1R activation in the basal state.[50–52]

Furthermore, GLP-1 has dual effects in β cells: stimulation of insulin secretion and a protective role in β cell survival and β cell mass in situations of cellular stress.[4] Indeed, GLP-1R activation has been reported to trigger the transcription of genes involved in proliferation or that display anti-apoptotic and/or anti-inflammatory activity.[4] One protein involved in GLP-1-induced β cell protection is CREB.[4,53] Here we report that only pharmacological concentrations of GLP-1 significantly activated CREB and that this effect is largely dependent on ARRB2. This was surprising because CREB was primarily found to be phosphorylated at S133 by PKA, which is similarly activated in *Arrb2*$^{+/+}$ and *Arrb2*$^{-/-}$ β cells upon pharmacological GLP-1 stimulation. Nevertheless, CREB is also activated by MSK1[41] and p90RSK,[41] two direct targets of ERK1/2 in the cytoplasm. When activated by ERK1/2, MSK1 and p90RSK may, in turn, phosphorylate nuclear targets such

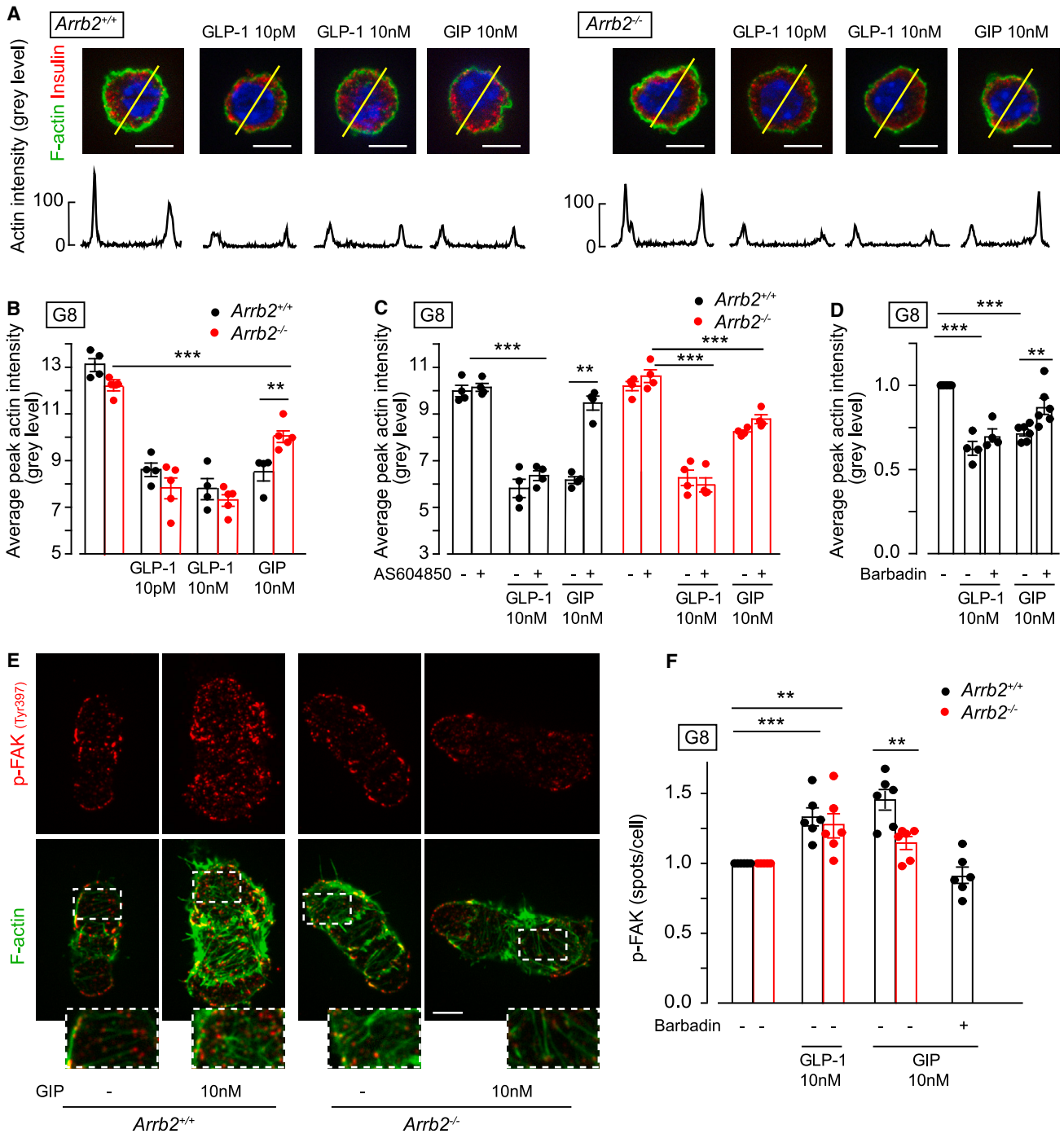


Figure 7. ARRB2 is required for F-actindepolymerization and FAK activation in response to GIP and seems to share a common pathway with PI3Kγ

(A) Representative images of dispersed mouse β cells incubated for 20 min in the absence or presence of GLP-1 or GIP, as indicated. Cells were stained for insulin (red), F-actin (green), and DAPI (blue). Intensity line scans for F-actin staining are shown at the bottom.

(B) Quantifications of average peak F-actin intensities from (A).

(C) Same as (B) except that β cells were pre-incubated for 2 h with a PI3Kγ inhibitor (1 μM AS604850) before being stimulated with GLP-1 and GIP.

(D) Same as (B) except that β cells were pre-incubated for 15 min with 30 μM barbadin before being stimulated with GLP-1 and GIP.

(E) Representative immunocytochemistry images of the phosphorylated form of FAK (p-FAK) at Tyr397 in dispersed islet cells. Insulin staining, to identify β cells, was also performed but was not imaged because the focal plane used did not ensure an appropriate focus for insulin (STAR Methods).

(F) Quantitative analysis of (E). Cells were in the presence of G8 in the absence or presence of GLP-1.

Scale bars, 5 μm. Data are mean ± SEM, n = 4–6 mice, one dot being the average of 40–50 cells from the same mouse. **p < 0.01, ***p < 0.001. One-way ANOVA followed by Sidak's post test.

as CREB. Therefore, decreased cytosolic ERK1/2 activity in *Arrb2*$^{-/-}$ β cells may be responsible for decreased CREB activation, as also reported for *Arrb2*$^{-/-}$ cystic fibrosis cells.[54] One could ask what impact deregulation of CREB activation may have. β cell-specific ablation of CREB in adult mice did not produce a major phenotype *in vivo* or on β cell mass unless the mice/islets were challenged with a high-fat diet or with a cocktail of cytokines,[53] respectively. We have reported previously[17] that *Arrb2*$^{-/-}$ mice had lower islet insulin content, decreased *Ins2* mRNA levels, and reduced β cell mass and plasticity on a high-fat diet associated with reduced proliferation. Furthermore, we observed an alteration of the insulin signaling pathway in islets in the absence of ARRB2.[17] Considering that ERK1/2 are involved in insulin gene expression[55] and that CREB induces the expression of IRS2,[56] an insulin signaling component involved in β cell survival, the reduced activation of ERK1/2 and CREB could potentially contribute, at least in part, to the deregulation of the β cell mass plasticity in *Arrb2*$^{-/-}$ mice.

Surprisingly, we observed that the contribution of ARRB2 to GIPR signaling was distinct from that of GLP-1R because ARRB2 is required for GIP potentiation of insulin secretion through F-actin depolymerization. Indeed, F-actin can act as a barrier by limiting insulin granule fusion with the plasma membrane. ARRB2 has been reported to interact with numerous proteins involved in cytoskeleton remodeling[57,58] and in actin reorganization.[9,58] ARRBs have also been reported to interact with and/or regulate the activity of members of the Rho family guanosine triphosphatases (GTPases) RhoA/Rac1/Cdc42,[59,60] with Rac1 and Cdc42 being involved in insulin granule trafficking and cytoskeletal rearrangement in β cells.[61] PI3Kγ, which is required for GIP- but not GLP-1-dependent insulin secretion via Rac1 activation[42] and actin depolymerization,[42] is also likely involved in this phenomenon. PI3Kγ, the only type 1B PI3K isoform, is activated by G-protein βγ subunits, whereas the most studied PI3Ks (type 1A) are activated through tyrosine kinase receptors. Nevertheless, while type1A PI3Ks interact with and are regulated by ARRBs,[9] the interaction/regulation of PI3Kγ by ARRBs has not yet been studied. We further report that ARRB2 is also involved in the activation of FAK and Paxillin in β cells upon GIP stimulation. FAK can regulate insulin secretion through actin remodeling[43,62] and granule trafficking[62] and has been reported to form a complex with ARRB2 to be recruited to GPCRs.[8] Additionally, inhibiting ARRB/β2-adaptin interaction with barbadin[8] abrogated FAK and Paxillin activation and decreased F-actin depolymerization upon GIP stimulation. Altogether, our data support the involvement of the ARRB2/FAK/Paxillin complex in the depolymerization of actin upon GIP stimulation. Furthermore, PI3K has also been reported to regulate FAK activity,[63,64] and some ARRB2 partners are also FAK partners (Src, mitogen-activated protein kinase [MAPK], PI3K, cytoskeleton proteins, etc.).[57] There are thus many points of molecular and functional convergence between ARRB2, PI3K, and FAK at the level of GPCRs, subcellular locations, partners, and associated signaling pathways/cellular processes.

Interestingly, the insulinotropic effect of the dual GLP-1/GIP agonist TZP does not require ARRB2 in mouse and human islets. Nevertheless, in human islets, it should be noted that, although not significant, the response to TZP is still lower in three of the four hARRB2-downregulated batches. This discrepancy in the effect of TZP in mouse versus human islets is consistent with the fact that TZP, which is imbalanced in favor of GIPR[6,40] in humans, has reduced potency in mice on GIPR favoring GLP-1R[6].

In T2D, the incretin pathway is disturbed with a decreased insulinotropic response to GIP but not necessarily to GLP-1.[1] *GLP1R* mRNA levels are decreased to some extent in T2D.[31,32] Despite decreased *Glp1r* mRNA levels in islets from metabolically stressed or diabetic rodents,[65–67] GLP-1R protein expression is unaltered.[67] This indicates that caution should be used when interpreting data for mRNA levels because they do not necessarily reflect protein expression.[67,68] In T2D, *GIPR mRNA* levels are barely affected,[31–33] while the GIPR protein level is uncertain because of a lack of suitable antibodies. ARRB2 protein expression is decreased in human islets treated under glucolipotoxic conditions. It is therefore tempting to speculate that decreased expression of ARRB2 in diabetic situations could contribute at least in part to the defect of insulin secretion in response to GIP in T2D.

Although GIP has been reported to play a role in β cell protection,[3,69] ARRB2 through ERK1/2 signaling does not seem to be involved because we observed similar ERK1/2 activity in *Arrb2*$^{+/+}$ and *Arrb2*$^{-/-}$ β cells. This is in agreement with a study reporting that ARRBs are not implicated in ERK1/2 recruitment upon GIP stimulation in HEK293 cells.[16] Therefore, other mechanisms should be involved in the β cell-protective role of GIP.

Finally, *Gipr* and *Arrb2* mRNA levels are expressed equally in rodent α and β cells[70,71], and glucagon released from α cells may act in a paracrine fashion on β cell GLP-1R.[72–74] One could imagine an indirect effect of GIP on α cells to regulate β cells. If we cannot exclude such a possibility, we believe that the majority of the effects that we observed with GIP are directly on GIPR in β cells. Indeed, (1) our experiments were performed with 8 mM glucose without a mixture of amino acids, and therefore glucagon secretion is not stimulated; (2) upon GIP stimulation, β cell signaling is distinct from that observed with GLP-1; (3) when ARRB2 was re-expressed in *Arrb2*$^{-/-}$ islets, it mostly occurred in β cells (STAR Methods and as reported for other adenoviruses[41]) and restored insulin secretion in response to GIP to similar levels than those from *Arrb2*$^{+/+}$ islets.

Conclusion

In conclusion, although GLP-1R has been studied more extensively than GIPR because of its therapeutic relevance, there is a renewed interest in GIPR, which has recently been proposed for therapeutic purposes as a dual and/or tri-agonist with GLP-1 and glucagon, respectively. We report that ARRB2 plays a distinct role in regulating GLP-1R and GIPR signaling in β cells, thus highlight the importance of evaluating the signaling pathways engaged by different agonists (biased or dual agonists) for future therapeutic purposes, taking into account the specific and non-redundant role of ARRB2. Indeed, the insulinotropic effect of the imbalanced dual GLP-1/GIP agonist TZP[6,40] was not dependent on ARRB2 expression. Our data report the possible functional consequences of decreased ARRB2 protein expression in pathological situations that should also be considered. The ability of many GPCRs to respond to ultralow concentrations of ligand suggests that a better understanding of this sensitivity is necessary for future research and drug discovery.

Limitations of the study

A limitation of this study is that the improvement of the incretin effect observed *in vivo* in *Arrb2*$^{-/-}$ mice could not be directly correlated with the enhanced insulin secretion *in vitro* in response to physiological concentrations of GLP-1. Because the *Arrb2* gene was inactivated in the whole organism and not conditionally in β cells, it is still possible that the enhanced incretin effect may be due to the absence of ARRB2 in cells other than pancreatic β cells. More *in vivo* studies and use of *Arrb2*$^{-/-}$ mice in which *Arrb2* is specifically inactivated in β cells would be needed.

Another limitation is that the majority of experiments were performed with mouse islet cells. Although decreased ARRB2 expression in human islets led to decreased insulin secretion in response to GIP, the underlying molecular mechanisms could not be investigated. Furthermore, while ARRB2 expression at the protein level is decreased under conditions mimicking T2D, we do not know whether this is also the case in islets from T2D donors.

STAR★METHODS

Detailed methods are provided in the online version of this paper and include the following:

- KEY RESOURCES TABLE
- RESOURCE AVAILABILITY
  - Lead contact
  - Materials availability
  - Data and code availability
- EXPERIMENTAL MODEL AND STUDY PARTICIPANT DETAILS
  - Mice
  - Human islets
- METHOD DETAILS
  - Human islet gene expression
  - Glucose tolerance test and plasma insulin measurements
  - Mouse islet isolation, cell culture and medium
  - Insulin secretion
  - Vectors, adenoviruses generation and adenoviral infection
  - cAMP, PKA, ERK1/2, $[Ca^{2+}]_{ER}$, DAG and $[Ca^{2+}]_c$ measurements
  - Total internal refection fluorescence (TIRF) microscopy
  - Immunofluorescence
  - Real-time quantitative RT-PCR
  - Western blotting
- QUANTIFICATION AND STATISTICAL ANALYSIS

SUPPLEMENTAL INFORMATION

Supplemental information can be found online at https://doi.org/10.1016/j.celrep.2023.113326.

ACKNOWLEDGMENTS

The authors thank J. Mateos-Langerak (MRI/Biocampus, Montpellier, France) for technical assistance with TIRF microscopy. The authors thank D. Greuet, M. Leportier, and S. Thirard (iExplore/Biocampus, Montpellier, France) for technical assistance with mice. The authors thank S. Granziera (LTCD, IRMB, CHU Montpellier, Montpellier, France) for assistance with providing human islets. The authors thank M. Leduc for assistance with adenovirus generation. This work was supported by the Centre National de la Recherche Scientifique, Institut National de la Santé et de la Recherche Médicale, Université de Montpellier, Fondation pour la Recherche Médicale (grant DRM20101220453), a research allocation from Société Francophone du Diabète (Allocation de recherche SFD 2020). P.G. was supported by grants from the FNRS (PDR T.0110.20) and the Pandarome project (40007487), which has received funding from the FWO and F.R.S.-FNRS under the Excellence of Science (EOS) program.

AUTHOR CONTRIBUTIONS

N.Z. and M.A.R. conceived the study and designed the experiments. N.Z., J.O., A.V., S.C., G.B., and M.A.R. performed the experiments. N.Z., J.O., A.V., S.C., and M.A.R. analyzed the experiments. J.S. and C.B. provided human islets. P.G. provided the D4ER adenovirus and participated in discussions. N.Z. and M.A.R. wrote the manuscript. All authors reviewed and approved the paper.

DECLARATION OF INTERESTS

The authors declare no competing interests.

Received: May 10, 2023
Revised: September 14, 2023
Accepted: October 7, 2023
Published: October 31, 2023

REFERENCES

1. Nauck, M.A., and Meier, J.J. (2018). Incretin hormones: Their role in health and disease. Diabetes Obes. Metabol. *20*, 5–21. https://doi.org/10.1111/dom.13129.
2. Ahren, B., Yamada, Y., and Seino, Y. (2020). The Incretin Effect in Female Mice With Double Deletion of GLP-1 and GIP Receptors. J Endocr Soc *4*, 1–11. https://doi.org/10.1210/jendso/bvz036.
3. Khan, R., Tomas, A., and Rutter, G.A. (2020). Effects on pancreatic Beta and other Islet cells of the glucose-dependent insulinotropic polypeptide. Peptides *125*, 170201–170208. https://doi.org/10.1016/j.peptides.2019.170201.
4. Costes, S., Bertrand, G., and Ravier, M.A. (2021). Mechanisms of Beta-Cell Apoptosis in Type 2 Diabetes-Prone Situations and Potential Protection by GLP-1-Based Therapies. Int. J. Mol. Sci. *22*, 5303–5323. https://doi.org/10.3390/ijms22105303.
5. Frías, J.P. (2020). Tirzepatide: a glucose-dependent insulinotropic polypeptide (GIP) and glucagon-like peptide-1 (GLP-1) dual agonist in development for the treatment of type 2 diabetes. Expet Rev. Endocrinol. Metabol. *15*, 379–394. https://doi.org/10.1080/17446651.2020.1830759.
6. El, K., Douros, J.D., Willard, F.S., Novikoff, A., Sargsyan, A., Perez-Tilve, D., Wainscott, D.B., Yang, B., Chen, A., Wothe, D., et al. (2023). The incretin co-agonist tirzepatide requires GIPR for hormone secretion from human islets. Nat. Metab. *5*, 945–954. https://doi.org/10.1038/s42255-023-00811-0.
7. Jones, B., Bloom, S.R., Buenaventura, T., Tomas, A., and Rutter, G.A. (2018). Control of insulin secretion by GLP-1. Peptides *100*, 75–84. https://doi.org/10.1016/j.peptides.2017.12.013.
8. Alexander, R.A., Lot, I., Saha, K., Abadie, G., Lambert, M., Decosta, E., Kobayashi, H., Beautrait, A., Borrull, A., Asnacios, A., et al. (2020). Beta-arrestins operate an on/off control switch for focal adhesion kinase activity. Cell. Mol. Life Sci. *77*, 5259–5279. https://doi.org/10.1007/s00018-020-03471-5.

9. DeFea, K.A. (2013). Arrestins in actin reorganization and cell migration. Prog. Mol. Biol. Transl. Sci. *118*, 205–222. https://doi.org/10.1016/B978-0-12-394440-5.00008-5.

10. Pydi, S.P., Barella, L.F., Zhu, L., Meister, J., Rossi, M., and Wess, J. (2022). beta-Arrestins as Important Regulators of Glucose and Energy Homeostasis. Annu. Rev. Physiol. *84*, 17–40. https://doi.org/10.1146/annurev-physiol-060721-092948.

11. Fletcher, M.M., Halls, M.L., Zhao, P., Clydesdale, L., Christopoulos, A., Sexton, P.M., and Wootten, D. (2018). Glucagon-like peptide-1 receptor internalisation controls spatiotemporal signalling mediated by biased agonists. Biochem. Pharmacol. *156*, 406–419. https://doi.org/10.1016/j.bcp.2018.09.003.

12. Roed, S.N., Nøhr, A.C., Wismann, P., Iversen, H., Bräuner-Osborne, H., Knudsen, S.M., and Waldhoer, M. (2015). Functional consequences of glucagon-like peptide-1 receptor cross-talk and trafficking. J. Biol. Chem. *290*, 1233–1243. https://doi.org/10.1074/jbc.M114.592436.

13. Jones, B., Buenaventura, T., Kanda, N., Chabosseau, P., Owen, B.M., Scott, R., Goldin, R., Angkathunyakul, N., Corrêa, I.R., Jr., Bosco, D., et al. (2018). Targeting GLP-1 receptor trafficking to improve agonist efficacy. Nat. Commun. *9*, 1602–1617. https://doi.org/10.1038/s41467-018-03941-2.

14. Jorgensen, R., Martini, L., Schwartz, T.W., and Elling, C.E. (2005). Characterization of glucagon-like peptide-1 receptor beta-arrestin 2 interaction: a high-affinity receptor phenotype. Mol. Endocrinol. *19*, 812–823. https://doi.org/10.1210/me.2004-0312.

15. Bitsi, S., El Eid, L., Manchanda, Y., Oqua, A.I., Mohamed, N., Hansen, B., Suba, K., Rutter, G.A., Salem, V., Jones, B., and Tomas, A. (2023). Divergent acute versus prolonged pharmacological GLP-1R responses in adult beta cell-specific beta-arrestin 2 knockout mice. Sci. Adv. *9*, eadf7737–23. https://doi.org/10.1126/sciadv.adf7737.

16. Jones, B., McGlone, E.R., Fang, Z., Pickford, P., Corrêa, I.R., Jr., Oishi, A., Jockers, R., Inoue, A., Kumar, S., Görlitz, F., et al. (2021). Genetic and biased agonist-mediated reductions in beta-arrestin recruitment prolong cAMP signalling at glucagon family receptors. J. Biol. Chem. *296*, 100133. https://doi.org/10.1074/jbc.RA120.016334.

17. Ravier, M.A., Leduc, M., Richard, J., Linck, N., Varrault, A., Pirot, N., Roussel, M.M., Bockaert, J., Dalle, S., and Bertrand, G. (2014). beta-Arrestin2 plays a key role in the modulation of the pancreatic beta cell mass in mice. Diabetologia *57*, 532–541. https://doi.org/10.1007/s00125-013-3130-7.

18. Zhu, L., Almaca, J., Dadi, P.K., Hong, H., Sakamoto, W., Rossi, M., Lee, R.J., Vierra, N.C., Lu, H., Cui, Y., et al. (2017). beta-arrestin-2 is an essential regulator of pancreatic beta-cell function under physiological and pathophysiological conditions. Nat. Commun. *8*, 1–18. https://doi.org/10.1038/ncomms14295.

19. Lin, Z., Zhao, Y., Song, L., Mu, K., Zhang, M., Liu, H., Li, X., Zhao, J., Wang, C., and Jia, W. (2016). Deletion of beta-Arrestin2 in mice limited pancreatic beta-cell expansion under metabolic stress through activation of JNK pathway. Mol. Med. *22*, 74–84. https://doi.org/10.2119/molmed.2015.00155.

20. Ismail, S., Dubois-Vedrenne, I., Laval, M., Tikhonova, I.G., D'Angelo, R., Sanchez, C., Clerc, P., Gherardi, M.J., Gigoux, V., Magnan, R., and Fourmy, D. (2015). Internalization and desensitization of the human glucose-dependent-insulinotropic receptor is affected by N-terminal acetylation of the agonist. Mol. Cell. Endocrinol. *414*, 202–215. https://doi.org/10.1016/j.mce.2015.07.001.

21. Al-Sabah, S., Al-Fulaij, M., Shaaban, G., Ahmed, H.A., Mann, R.J., Donnelly, D., Bünemann, M., and Krasel, C. (2014). The GIP receptor displays higher basal activity than the GLP-1 receptor but does not recruit GRK2 or arrestin3 effectively. PLoS One *9*, e106890–e106898. https://doi.org/10.1371/journal.pone.0106890.

22. Gabe, M.B.N., Sparre-Ulrich, A.H., Pedersen, M.F., Gasbjerg, L.S., Inoue, A., Bräuner-Osborne, H., Hartmann, B., and Rosenkilde, M.M. (2018). Human GIP(3-30)NH2 inhibits G protein-dependent as well as G protein-independent signaling and is selective for the GIP receptor with high-affinity binding to primate but not rodent GIP receptors. Biochem. Pharmacol. *150*, 97–107. https://doi.org/10.1016/j.bcp.2018.01.040.

23. Abdullah, N., Beg, M., Soares, D., Dittman, J.S., and McGraw, T.E. (2016). Downregulation of a GPCR by beta-Arrestin2-Mediated Switch from an Endosomal to a TGN Recycling Pathway. Cell Rep. *17*, 2966–2978. https://doi.org/10.1016/j.celrep.2016.11.050.

24. Yuliantie, E., Darbalaei, S., Dai, A., Zhao, P., Yang, D., Sexton, P.M., Wang, M.W., and Wootten, D. (2020). Pharmacological characterization of mono- dual- and tri-peptidic agonists at GIP and GLP-1 receptors. Biochem. Pharmacol. *177*, 114001–114013. https://doi.org/10.1016/j.bcp.2020.114001.

25. Shigeto, M., Ramracheya, R., Tarasov, A.I., Cha, C.Y., Chibalina, M.V., Hastoy, B., Philippaert, K., Reinbothe, T., Rorsman, N., Salehi, A., et al. (2015). GLP-1 stimulates insulin secretion by PKC-dependent TRPM4 and TRPM5 activation. J. Clin. Invest. *125*, 4714–4728. https://doi.org/10.1172/JCI81975.

26. Lebreton, F., Pirog, A., Belouah, I., Bosco, D., Berney, T., Meda, P., Bornat, Y., Catargi, B., Renaud, S., Raoux, M., and Lang, J. (2015). Slow potentials encode intercellular coupling and insulin demand in pancreatic beta cells. Diabetologia *58*, 1291–1299. https://doi.org/10.1007/s00125-015-3558-z.

27. Bak, M.J., Wewer Albrechtsen, N.J., Pedersen, J., Knop, F.K., Vilsbøll, T., Jørgensen, N.B., Hartmann, B., Deacon, C.F., Dragsted, L.O., and Holst, J.J. (2014). Specificity and sensitivity of commercially available assays for glucagon-like peptide-1 (GLP-1): implications for GLP-1 measurements in clinical studies. Diabetes Obes. Metabol. *16*, 1155–1164. https://doi.org/10.1111/dom.12352.

28. Kothare, P.A., Linnebjerg, H., Isaka, Y., Uenaka, K., Yamamura, A., Yeo, K.P., de la Peña, A., Teng, C.H., Mace, K., Fineman, M., et al. (2008). Pharmacokinetics, pharmacodynamics, tolerability, and safety of exenatide in Japanese patients with type 2 diabetes mellitus. J. Clin. Pharmacol. *48*, 1389–1399. https://doi.org/10.1177/0091270008323750.

29. Calara, F., Taylor, K., Han, J., Zabala, E., Carr, E.M., Wintle, M., and Fineman, M. (2005). A randomized, open-label, crossover study examining the effect of injection site on bioavailability of exenatide (synthetic exendin-4). Clin. Therapeut. *27*, 210–215. https://doi.org/10.1016/j.clinthera.2005.02.008.

30. Alonso, L., Piron, A., Moran, I., Guindo-Martinez, M., Bonas-Guarch, S., Atla, G., Miguel-Escalada, I., Royo, R., Puiggros, M., Garcia-Hurtado, X., et al. (2021). TIGER: The gene expression regulatory variation landscape of human pancreatic islets. Cell Rep. *37*, 1–15. https://doi.org/10.1016/j.celrep.2021.109807.

31. Solimena, M., Schulte, A.M., Marselli, L., Ehehalt, F., Richter, D., Kleeberg, M., Mziaut, H., Knoch, K.P., Parnis, J., Bugliani, M., et al. (2018). Systems biology of the IMIDIA biobank from organ donors and pancreatectomised patients defines a novel transcriptomic signature of islets from individuals with type 2 diabetes. Diabetologia *61*, 641–657. https://doi.org/10.1007/s00125-017-4500-3.

32. Taneera, J., Lang, S., Sharma, A., Fadista, J., Zhou, Y., Ahlqvist, E., Jonsson, A., Lyssenko, V., Vikman, P., Hansson, O., et al. (2012). A systems genetics approach identifies genes and pathways for type 2 diabetes in human islets. Cell Metabol. *16*, 122–134. https://doi.org/10.1016/j.cmet.2012.06.006.

33. Marselli, L., Thorne, J., Dahiya, S., Sgroi, D.C., Sharma, A., Bonner-Weir, S., Marchetti, P., and Weir, G.C. (2010). Gene expression profiles of Beta-cell enriched tissue obtained by laser capture microdissection from subjects with type 2 diabetes. PLoS One *5*, e11499. https://doi.org/10.1371/journal.pone.0011499.

34. Cnop, M., Abdulkarim, B., Bottu, G., Cunha, D.A., Igoillo-Esteve, M., Masini, M., Turatsinze, J.V., Griebel, T., Villate, O., Santin, I., et al. (2014). RNA sequencing identifies dysregulation of the human pancreatic islet transcriptome by the saturated fatty acid palmitate. Diabetes *63*, 1978–1993. https://doi.org/10.2337/db13-1383.

35. Luan, B., Zhao, J., Wu, H., Duan, B., Shu, G., Wang, X., Li, D., Jia, W., Kang, J., and Pei, G. (2009). Deficiency of a beta-arrestin-2 signal complex contributes to insulin resistance. Nature *457*, 1146–1149. https://doi.org/10.1038/nature07617.

36. Zhang, M., Zhu, Y., Mu, K., Li, L., Lu, J., Zhao, J., Huang, X., Wang, C., and Jia, W. (2013). Loss of beta-arrestin2 mediates pancreatic-islet dysfunction in mice. Biochem. Biophys. Res. Commun. *435*, 345–349. https://doi.org/10.1016/j.bbrc.2013.04.079.

37. Holst, J.J. (2019). The incretin system in healthy humans: The role of GIP and GLP-1. Metabolism *96*, 46–55. https://doi.org/10.1016/j.metabol.2019.04.014.

38. Balas, B., Baig, M.R., Watson, C., Dunning, B.E., Ligueros-Saylan, M., Wang, Y., He, Y.L., Darland, C., Holst, J.J., Deacon, C.F., et al. (2007). The dipeptidyl peptidase IV inhibitor vildagliptin suppresses endogenous glucose production and enhances islet function after single-dose administration in type 2 diabetic patients. J. Clin. Endocrinol. Metab. *92*, 1249–1255. https://doi.org/10.1210/jc.2006-1882.

39. Moens, K., Heimberg, H., Flamez, D., Huypens, P., Quartier, E., Ling, Z., Pipeleers, D., Gremlich, S., Thorens, B., and Schuit, F. (1996). Expression and functional activity of glucagon, glucagon-like peptide I, and glucose-dependent insulinotropic peptide receptors in rat pancreatic islet cells. Diabetes *45*, 257–261. https://doi.org/10.2337/diab.45.2.257.

40. Willard, F.S., Douros, J.D., Gabe, M.B., Showalter, A.D., Wainscott, D.B., Suter, T.M., Capozzi, M.E., van der Velden, W.J., Stutsman, C., Cardona, G.R., et al. (2020). Tirzepatide is an imbalanced and biased dual GIP and GLP-1 receptor agonist. JCI Insight *5*, e140532. https://doi.org/10.1172/jci.insight.140532.

41. Leduc, M., Richard, J., Costes, S., Muller, D., Varrault, A., Compan, V., Mathieu, J., Tanti, J.F., Pagès, G., Pouyssegur, J., et al. (2017). ERK1 is dispensable for mouse pancreatic beta cell function but is necessary for glucose-induced full activation of MSK1 and CREB. Diabetologia *60*, 1999–2010. https://doi.org/10.1007/s00125-017-4356-6.

42. Kolic, J., Spigelman, A.F., Smith, A.M., Manning Fox, J.E., and MacDonald, P.E. (2014). Insulin secretion induced by glucose-dependent insulinotropic polypeptide requires phosphatidylinositol 3-kinase gamma in rodent and human beta-cells. J. Biol. Chem. *289*, 32109–32120. https://doi.org/10.1074/jbc.M114.577510.

43. Rondas, D., Tomas, A., Soto-Ribeiro, M., Wehrle-Haller, B., and Halban, P.A. (2012). Novel mechanistic link between focal adhesion remodeling and glucose-stimulated insulin secretion. J. Biol. Chem. *287*, 2423–2436. https://doi.org/10.1074/jbc.M111.279885.

44. Pydi, S.P., Jain, S., Tung, W., Cui, Y., Zhu, L., Sakamoto, W., Jain, S., Abel, B.S., Skarulis, M.C., Liu, J., et al. (2019). Adipocyte beta-arrestin-2 is essential for maintaining whole body glucose and energy homeostasis. Nat. Commun. *10*, 2936. https://doi.org/10.1038/s41467-019-11003-4.

45. Zhu, L., Rossi, M., Cui, Y., Lee, R.J., Sakamoto, W., Perry, N.A., Urs, N.M., Caron, M.G., Gurevich, V.V., Godlewski, G., et al. (2017). Hepatic beta-arrestin 2 is essential for maintaining euglycemia. J. Clin. Invest. *127*, 2941–2945. https://doi.org/10.1172/JCI92913.

46. Civciristov, S., Ellisdon, A.M., Suderman, R., Pon, C.K., Evans, B.A., Kleifeld, O., Charlton, S.J., Hlavacek, W.S., Canals, M., and Halls, M.L. (2018). Preassembled GPCR signaling complexes mediate distinct cellular responses to ultralow ligand concentrations. Sci. Signal. *11*, eaan1188–22. https://doi.org/10.1126/scisignal.aan1188.

47. Villanueva-Peñacarrillo, M.L., Márquez, L., González, N., Díaz-Miguel, M., and Valverde, I. (2001). Effect of GLP-1 on lipid metabolism in human adipocytes. Horm. Metab. Res. *33*, 73–77. https://doi.org/10.1055/s-2001-12428.

48. Cahill, T.J., 3rd, Thomsen, A.R.B., Tarrasch, J.T., Plouffe, B., Nguyen, A.H., Yang, F., Huang, L.Y., Kahsai, A.W., Bassoni, D.L., Gavino, B.J., et al. (2017). Distinct conformations of GPCR-beta-arrestin complexes mediate desensitization, signaling, and endocytosis. Proc. Natl. Acad. Sci. USA *114*, 2562–2567. https://doi.org/10.1073/pnas.1701529114.

49. Kuna, R.S., Girada, S.B., Asalla, S., Vallentyne, J., Maddika, S., Patterson, J.T., Smiley, D.L., Dimarchi, R.D., and Mitra, P. (2013). Glucagon-like peptide-1 receptor-mediated endosomal cAMP generation promotes glucose-stimulated insulin secretion in pancreatic beta-cells. Am. J. Physiol. Endocrinol. Metab. *305*, E161–E170. https://doi.org/10.1152/ajpendo.00551.2012.

50. Shuai, H., Xu, Y., Ahooghalandari, P., and Tengholm, A. (2021). Glucose-induced cAMP elevation in beta-cells involves amplification of constitutive and glucagon-activated GLP-1 receptor signalling. Acta Physiol. *231*, e13611–e13615. https://doi.org/10.1111/apha.13611.

51. Marchetti, P., Bugliani, M., Boggi, U., Masini, M., and Marselli, L. (2012). The pancreatic beta cells in human type 2 diabetes. Adv. Exp. Med. Biol. *771*, 288–309. https://doi.org/10.1007/978-1-4614-5441-0_22.

52. Traub, S., Meier, D.T., Schulze, F., Dror, E., Nordmann, T.M., Goetz, N., Koch, N., Dalmas, E., Stawiski, M., Makshana, V., et al. (2017). Pancreatic alpha Cell-Derived Glucagon-Related Peptides Are Required for beta Cell Adaptation and Glucose Homeostasis. Cell Rep. *18*, 3192–3203. https://doi.org/10.1016/j.celrep.2017.03.005.

53. Shin, S., Le Lay, J., Everett, L.J., Gupta, R., Rafiq, K., and Kaestner, K.H. (2014). CREB mediates the insulinotropic and anti-apoptotic effects of GLP-1 signaling in adult mouse beta-cells. Mol. Metabol. *3*, 803–812. https://doi.org/10.1016/j.molmet.2014.08.001.

54. Manson, M.E., Corey, D.A., Rymut, S.M., and Kelley, T.J. (2011). beta-arrestin-2 regulation of the cAMP response element binding protein. Biochemistry *50*, 6022–6029. https://doi.org/10.1021/bi200015h.

55. Lawrence, M., Shao, C., Duan, L., McGlynn, K., and Cobb, M.H. (2008). The protein kinases ERK1/2 and their roles in pancreatic beta cells. Acta Physiol. *192*, 11–17. https://doi.org/10.1111/j.1748-1716.2007.01785.x.

56. Jhala, U.S., Canettieri, G., Screaton, R.A., Kulkarni, R.N., Krajewski, S., Reed, J., Walker, J., Lin, X., White, M., and Montminy, M. (2003). cAMP promotes pancreatic beta-cell survival via CREB-mediated induction of IRS2. Genes Dev. *17*, 1575–1580. https://doi.org/10.1101/gad.1097103.

57. Xiao, K., McClatchy, D.B., Shukla, A.K., Zhao, Y., Chen, M., Shenoy, S.K., Yates, J.R., 3rd, and Lefkowitz, R.J. (2007). Functional specialization of beta-arrestin interactions revealed by proteomic analysis. Proc. Natl. Acad. Sci. USA *104*, 12011–12016. https://doi.org/10.1073/pnas.0704849104.

58. Szenasi, T., Turu, G., and Hunyady, L. (2023). Interactions between beta-arrestin proteins and the cytoskeletal system, and their relevance to neurodegenerative disorders. Front. Endocrinol. *14*, 1–10. https://doi.org/10.3389/fendo.2023.957981.

59. Cleghorn, W.M., Bulus, N., Kook, S., Gurevich, V.V., Zent, R., and Gurevich, E.V. (2018). Non-visual arrestins regulate the focal adhesion formation via small GTPases RhoA and Rac1 independently of GPCRs. Cell. Signal. *42*, 259–269. https://doi.org/10.1016/j.cellsig.2017.11.003.

60. Laporte, S.A., and Scott, M.G.H. (2019). beta-Arrestins: Multitask Scaffolds Orchestrating the Where and When in Cell Signalling. Methods Mol. Biol. *1957*, 9–55. https://doi.org/10.1007/978-1-4939-9158-7_2.

61. Veluthakal, R., and Thurmond, D.C. (2021). Emerging Roles of Small GTPases in Islet beta-Cell Function. Cells *10*, 1503–1524. https://doi.org/10.3390/cells10061503.

62. Cai, E.P., Casimir, M., Schroer, S.A., Luk, C.T., Shi, S.Y., Choi, D., Dai, X.Q., Hajmrle, C., Spigelman, A.F., Zhu, D., et al. (2012). In vivo role of focal adhesion kinase in regulating pancreatic beta-cell mass and function through insulin signaling, actin dynamics, and granule trafficking. Diabetes *61*, 1708–1718. https://doi.org/10.2337/db11-1344.

63. Bellas, R.E., Harrington, E.O., Sheahan, K.L., Newton, J., Marcus, C., and Rounds, S. (2002). FAK blunts adenosine-homocysteine-induced endothelial cell apoptosis: requirement for PI 3-kinase. Am. J. Physiol. Lung Cell Mol. Physiol. *282*, L1135–L1142. https://doi.org/10.1152/ajplung.00174.2001.

64. Sonoda, Y., Watanabe, S., Matsumoto, Y., Aizu-Yokota, E., and Kasahara, T. (1999). FAK is the upstream signal protein of the phosphatidylinositol

3-kinase-Akt survival pathway in hydrogen peroxide-induced apoptosis of a human glioblastoma cell line. J. Biol. Chem. *274*, 10566–10570. https://doi.org/10.1074/jbc.274.15.10566.

65. Xu, G., Kaneto, H., Laybutt, D.R., Duvivier-Kali, V.F., Trivedi, N., Suzuma, K., King, G.L., Weir, G.C., and Bonner-Weir, S. (2007). Downregulation of GLP-1 and GIP receptor expression by hyperglycemia: possible contribution to impaired incretin effects in diabetes. Diabetes *56*, 1551–1558. https://doi.org/10.2337/db06-1033.
66. Piteau, S., Olver, A., Kim, S.J., Winter, K., Pospisilik, J.A., Lynn, F., Manhart, S., Demuth, H.U., Speck, M., Pederson, R.A., and McIntosh, C.H.S. (2007). Reversal of islet GIP receptor down-regulation and resistance to GIP by reducing hyperglycemia in the Zucker rat. Biochem. Biophys. Res. Commun. *362*, 1007–1012. https://doi.org/10.1016/j.bbrc.2007.08.115.
67. Gray, S.M., Xin, Y., Ross, E.C., Chazotte, B.M., Capozzi, M.E., El, K., Svendsen, B., Ravn, P., Sloop, K.W., Tong, J., et al. (2020). Discordance between GLP-1R gene and protein expression in mouse pancreatic islet cells. J. Biol. Chem. *295*, 11529–11541. https://doi.org/10.1074/jbc.RA120.014368.
68. Ruiz, L., Gurlo, T., Ravier, M.A., Wojtusciszyn, A., Mathieu, J., Brown, M.R., Broca, C., Bertrand, G., Butler, P.C., Matveyenko, A.V., et al. (2018). Proteasomal degradation of the histone acetyl transferase p300 contributes to beta-cell injury in a diabetes environment. Cell Death Dis. *9*, 600–612. https://doi.org/10.1038/s41419-018-0603-0.
69. Campbell, J.E., Ussher, J.R., Mulvihill, E.E., Kolic, J., Baggio, L.L., Cao, X., Liu, Y., Lamont, B.J., Morii, T., Streutker, C.J., et al. (2016). TCF1 links GIPR signaling to the control of beta cell function and survival. Nat. Med. *22*, 84–90. https://doi.org/10.1038/nm.3997.
70. DiGruccio, M.R., Mawla, A.M., Donaldson, C.J., Noguchi, G.M., Vaughan, J., Cowing-Zitron, C., van der Meulen, T., and Huising, M.O. (2016). Comprehensive alpha, beta and delta cell transcriptomes reveal that ghrelin selectively activates delta cells and promotes somatostatin release from pancreatic islets. Mol. Metabol. *5*, 449–458. https://doi.org/10.1016/j.molmet.2016.04.007.
71. Adriaenssens, A.E., Svendsen, B., Lam, B.Y.H., Yeo, G.S.H., Holst, J.J., Reimann, F., and Gribble, F.M. (2016). Transcriptomic profiling of pancreatic alpha, beta and delta cell populations identifies delta cells as a principal target for ghrelin in mouse islets. Diabetologia *59*, 2156–2165. https://doi.org/10.1007/s00125-016-4033-1.
72. Zhu, L., Dattaroy, D., Pham, J., Wang, L., Barella, L.F., Cui, Y., Wilkins, K.J., Roth, B.L., Hochgeschwender, U., Matschinsky, F.M., et al. (2019). Intra-islet glucagon signaling is critical for maintaining glucose homeostasis. JCI Insight *5*, e127994. https://doi.org/10.1172/jci.insight.127994.
73. Capozzi, M.E., Svendsen, B., Encisco, S.E., Lewandowski, S.L., Martin, M.D., Lin, H., Jaffe, J.L., Coch, R.W., Haldeman, J.M., MacDonald, P.E., et al. (2019). beta Cell tone is defined by proglucagon peptides through cAMP signaling. JCI Insight *4*, e126742. https://doi.org/10.1172/jci.insight.126742.
74. Svendsen, B., Larsen, O., Gabe, M.B.N., Christiansen, C.B., Rosenkilde, M.M., Drucker, D.J., and Holst, J.J. (2018). Insulin Secretion Depends on Intra-islet Glucagon Signaling. Cell Rep. *25*, 1127–1134.e2. https://doi.org/10.1016/j.celrep.2018.10.018.
75. Nikolaev, V.O., Bünemann, M., Hein, L., Hannawacker, A., and Lohse, M.J. (2004). Novel single chain cAMP sensors for receptor-induced signal propagation. J. Biol. Chem. *279*, 37215–37218. https://doi.org/10.1074/jbc.C400302200.
76. Allen, M.D., and Zhang, J. (2006). Subcellular dynamics of protein kinase A activity visualized by FRET-based reporters. Biochem. Biophys. Res. Commun. *348*, 716–721. https://doi.org/10.1016/j.bbrc.2006.07.136.
77. Li, Y., Asuri, S., Rebhun, J.F., Castro, A.F., Paranavitana, N.C., and Quilliam, L.A. (2006). The RAP1 guanine nucleotide exchange factor Epac2 couples cyclic AMP and Ras signals at the plasma membrane. J. Biol. Chem. *281*, 2506–2514. https://doi.org/10.1074/jbc.M508165200.
78. Scott, M.G.H., Benmerah, A., Muntaner, O., and Marullo, S. (2002). Recruitment of activated G protein-coupled receptors to pre-existing clathrin-coated pits in living cells. J. Biol. Chem. *277*, 3552–3559. https://doi.org/10.1074/jbc.M106586200.
79. Ravier, M.A., Daro, D., Roma, L.P., Jonas, J.C., Cheng-Xue, R., Schuit, F.C., and Gilon, P. (2011). Mechanisms of control of the free Ca^{2+} concentration in the endoplasmic reticulum of mouse pancreatic beta-cells: interplay with cell metabolism and $[Ca^{2+}]_c$ and role of SERCA2b and SERCA3. Diabetes *60*, 2533–2545. https://doi.org/10.2337/db10-1543.
80. Pinton, P., Tsuboi, T., Ainscow, E.K., Pozzan, T., Rizzuto, R., and Rutter, G.A. (2002). Dynamics of glucose-induced membrane recruitment of protein kinase C beta II in living pancreatic islet beta-cells. J. Biol. Chem. *277*, 37702–37710. https://doi.org/10.1074/jbc.M204478200.
81. Diraison, F., Parton, L., Ferré, P., Foufelle, F., Briscoe, C.P., Leclerc, I., and Rutter, G.A. (2004). Over-expression of sterol-regulatory-element-binding protein-1c (SREBP1c) in rat pancreatic islets induces lipogenesis and decreases glucose-stimulated insulin release: modulation by 5-aminoimidazole-4-carboxamide ribonucleoside (AICAR). Biochem. J. *378*, 769–778. https://doi.org/10.1042/BJ20031277.
82. Luo, J., Deng, Z.L., Luo, X., Tang, N., Song, W.X., Chen, J., Sharff, K.A., Luu, H.H., Haydon, R.C., Kinzler, K.W., et al. (2007). A protocol for rapid generation of recombinant adenoviruses using the AdEasy system. Nat. Protoc. *2*, 1236–1247. https://doi.org/10.1038/nprot.2007.135.
83. Calebiro, D., Nikolaev, V.O., and Lohse, M.J. (2010). Imaging of persistent cAMP signaling by internalized G protein-coupled receptors. J. Mol. Endocrinol. *45*, 1–8. https://doi.org/10.1677/JME-10-0014.
84. Vandesompele, J., De Preter, K., Pattyn, F., Poppe, B., Van Roy, N., De Paepe, A., and Speleman, F. (2002). Accurate normalization of real-time quantitative RT-PCR data by geometric averaging of multiple internal control genes. Genome Biol. *3*, RESEARCH0034. https://doi.org/10.1186/gb-2002-3-7-research0034.

STAR★METHODS

KEY RESOURCES TABLE

REAGENT or RESOURCE	SOURCE	IDENTIFIER
Antibodies		
Insulin	Abcam	ab7842; RRID:AB_306130
Phospho-ERK1/2 (Thr202/Tyr204)	Cell Signaling	#9101; RRID:AB_331646
Phospho-CREB (Ser133)	Millipore	06519; RRID:AB_310153
Phospho-FAK (Tyr397)	Cell Signaling	#3283; RRID:AB_2173659
Phospho-Paxillin (Tyr118)	Cell Signaling	#2541; RRID:AB_2174466
Cy3-affiniPure Donkey anti-rabbit	Jackson Immunoresearch	711-166-152; RRID:AB_2313568
Cy3-affiniPure Donkey anti-guinea pig	Jackson Immunoresearch	706-165-148; RRID:AB_2340460
Alexa Fluor 680 Donkey anti-guinea pig	Jackson Immunoresearch	706-625-148; RRID:AB_2340478
Alexa Fluor 488 Donkey anti-guinea pig	Jackson Immunoresearch	706-546-148; RRID:AB_2340473
ARRB2	Abcam	ab54790; RRID:AB_2060273
GAPDH	Cell Signaling	#5174; RRID:AB_10622025
Cleaved Casp-3	Cell Signaling	#9661; RRID:AB_2341188
Anti Rabbit IgG HRP	Ozyme	CST7074; RRID:AB_2099233
Anti mouse IgG HRP	Ozyme	CST7076s; RRID:AB_330924
Bacterial and virus strains		
Human Adenovirus Type5 (dE1/E3) for expressing human ShRNA	Vector Biolabs	This study
Human Adenovirus Type5 (dE1/E3) for other adenoviruses	Our lab	This study
BJ5183-AD-1	Agilent	200157
Biological samples		
Human islets	Laboratory of cell Therapy for diabetes (PRIMS platform)	https://www.ilots-montpellier.fr/
Chemicals, peptides, and recombinant proteins		
GLP-1 (7–36 amide)	BACHEM	4030663
hGIP	BACHEM	4030658
Forskolin	Sigma-Aldrich	F6886
AS-604850	Selleckchem	S2681
Barbadin	Axon MedChem	2774
CMRL 1066	Life Technologies	21530027
D- + -glucose	Sigma-Aldrich	G7528
FBS	Life Technologies	10270106
L-glutamine	Life Technologies	25030024
100 IU/mL penicillin 100 μg/mL streptomycin	Life Technologies	15140122
Dithizone	Sigma-Aldrich	D5130
Sodium palmitate	Sigma-Aldrich	P9767
BSA-Free fatty acid	Sigma-Aldrich	A8806
RPMI-1640	Life Technologies	31870025
Tirzepatide	MedChemExpress	HY-P1731B
Trypsin-EDTA	Life Technologies	25200056
BSA	Sigma-Aldrich	A8022
Phusion High Fidelity polymerase	Thermo Scientific	F530S
Fura-2 Leakage Resistant-AM	Interchim	FP-AM603A
EGTA	Sigma-Aldrich	E4378
Formaldehyde	Sigma-Aldrich	252549

(*Continued on next page*)

Continued

REAGENT or RESOURCE	SOURCE	IDENTIFIER
NaF	Sigma-Aldrich	S1504
DAPI	Roche	10236276001
Collagenase	Sigma-Aldrich	C9263
MoMuLVRT	Life Technologies	28025013
SybrGreen Master Mix	Roche	4887352001
DPBS	Sigma-Aldrich	D8662
NuPAGE gel	Termo Fisher Scientific	NP0321BOX
Membrane FluoroTrans W PVDF 0.2μ	VWR	516–0249
Immobilon western Chemilum HRP substrate	Sigma-Aldrich	WBKLS0100
Critical commercial assays		
KAPA mouse genotyping kit	Sigma-Aldrich	KK7302
Mouse insulin ultra-sensitive ELISA	Crystal Chem	90080
Mouse glucagon ELISA	Crystal Chem	81518
Mouse GLP-1 ELISA (total)	Crystal Chem	81508
Mouse active GIP ELISA	Crystal Chem	81511
Insulin ultra sensitive kit	PerkinElmer/Cisbio	62IN2PEH
RNAeasy microkit	Qiagen	74004
Upward DAG	Montana Molecular	U0300G-005
Deposited data		
Transcriptomic datasets from human pancreatic islets	[31,32,33]	GSE76894; GSE38642; GSE20966
Experimental models: Cell lines		
HEK293 cells	ATCC	CRL-1573
Experimental models: Organisms/strains		
Arrb2tm1Rjl/J	Laboratory of R. J. Lefkowitz, Duke University Medical Center, Durham, NC, USA	RRID:IMSR_JAX:011130
Oligonucleotides		
Primers for real-time quantitative RT-PCR, See Table S1	This study	N/A
Recombinant DNA		
pCMV-EPAC2B-camps	V. Nikolaev	[75]
pShuttle-CMV	M.A. Ravier	N/A
pCMV-AKAR3	J. Zhang	[76]
pCMV-EGFP-EPAC2	L. Quilliam	[77]
pCMV-ARRB2-GFP	M Scott	[78]
pCMV-cytoEKAR	Addgene	18679,[41]
pCMV-D4ER	P. Gilon M.A. Ravier	[79]
pCMV-PKCβII	G.A. Rutter	[80]
mCherry-U6-h-ARRB2-shRNA	Vector Biolabs	#shADV-201476
mCherry-U6-scrmb-shRNA	Vector Biolabs	#1781
Software and algorithms		
MetaFluor® software	Molecular devices	https://www.moleculardevices.com
ImageJ	ImageJ	https://imagej-nih-gov.proxy.insermbiblio.inist.fr/ij/index.htm
ZenBlue software	Zeiss	https://www.zeiss.com
GraphPad Prism 9.2.0	GraphPad	https://www.graphpad.com
geNorm_3.4	geNorm	https://genorm.cmgg.be/

(*Continued on next page*)

Continued

REAGENT or RESOURCE	SOURCE	IDENTIFIER
Other		
FreeStyle Optium *Neo* glucometer	Abbott	https://www.freestyle.abbott/fr-fr/accueil.html

RESOURCE AVAILABILITY

Lead contact

Further information and request for reagents and resources should be directed to and will be fulfilled by the lead contact, Dr Magalie A Ravier (magalie.ravier@igf.cnrs.fr).

Materials availability

All materials generated in this study are available from the lead contact with a completed Materials Transfer Agreement.

Data and code availability

- This paper analyzes existing, publicly available data. These accession numbers for the datasets are listed in the key resources table. All data reported in this paper will be shared by the lead contract upon request.
- This paper does not report original code.
- Any additional information required to reanalyze the data reported in this paper is available from the lead contact upon request.

EXPERIMENTAL MODEL AND STUDY PARTICIPANT DETAILS

Mice

Mice were maintained according to European Union guidelines for the use of laboratory animals. Studies complied with the animal welfare guidelines of the European Community (EU directive 2010/63/EU) and was approved by the ethic committee (CEEA N°36) and the ministry of education and research, France (D34-172-41). Mice were housed in pathogen free animal house, with a 12light/12dark cycle, with a temperature of 20°C, and had freely access to food (4% Fat diet) and water. All experiments were performed using 4-5 month-old male mice.

The strain of the mice is Arrb2tm1Rjl/J. As already reported,[17] the heterozygous (referred as *Arrb2*$^{+/-}$) mice were obtained from R. J. Lefkowitz (Duke University Medical Center, Durham, NC, USA). Mice were subsequently backcrossed onto C57BL/6J background (Charles River, Lyon, France). *Arrb2*$^{-/-}$ mice and their wild-type littermates (*Arrb2*$^{+/+}$) were generated by breeding heterozygous animals, and genotyping was performed by PCR.[17] In agreement with our previous study,[17] *Arrb2*$^{-/-}$ mice display similar body weight than *Arrb2*$^{+/+}$ mice (32.78 ± 1.03 vs. 33.64 ± 1.71 g, respectively, n = 10) but significant increased fed blood glucose levels (10.09 ± 0.33 vs. 8.39 ± 0.67 mM, *p < 0.05, respectively, n = 10).

Human islets

Experiments involving human islets were performed in agreement with the local ethic committee (Biological Ressources center, Collection 5 "Human Islets of Langerhans", 345 identifiant Biobanque n° BB-0033-00031, CHU, Montpellier), the institutional ethical committee of the French Agence de la Biomédecine (ABM n° PFS 13-008) and the French Ministry of Research (DC-2011-1401 and AC-2017-3039). Informed consent was obtained from family for all pancreases. Pancreases were harvested from thirteen brain-dead non-diabetic donors. None of them had history of diabetes. Below are listed, for each donor, in this order: unique identifier (HM)/donor age (years)/sex (M/F), donor BMI (kg/m^2).

Figure 1B:
HM78/50/F/29.
HM85/56/M/22.
HM87/77/F/31.
HM71/67/F/25.
HM72/65/F/21.
Figure 1C:
HM50/66/M/30.
HM52/74/F/29.
HM54/36/M/23.
HM66/68/M/30.
Figures 6A–6C.
HM95/60/M/29.

HM97/37/M/26.
HM108/56/F/24.
HM111/55/M/25.

Isolated islets were prepared by collagenase digestion followed by density gradient purification at the Laboratory of Cell Therapy for Diabetes (PRIMS platform).[68] Following isolation, human islets were cultured for recovery for 3 days at 37°C, in a 5% CO2 atmosphere, in CMRL 1066 medium (Life Technologies) containing 5.6 mM glucose supplemented with 10% FBS, 2 mM glutamine, 100 IU/mL penicillin, and 100 μg/mL streptomycin. The islet purity was 90%, as re-assessed by dithizone staining in the host laboratory. Islets were then incubated for 72 h in CMRL 1066 medium containing either 5.6 mM glucose, 30 mM glucose ±0.5 mM palmitate,[68] or 5.6 mM glucose supplemented with the adenoviruses ShRNA-hARRB2 or ShRNA-scramble.

METHOD DETAILS

Human islet gene expression

GEO accession number (GEO: GSE76894,[31] GSE38642,[32] GSE20966,[33]) were encoded in GEO from NCBI. Transcriptomic datasets from human pancreatic islets were downloaded from GEO2R. Adjusted p values (multiple-testing corrections) for microarray analysis were either reported by the TIGER resource (https://tiger.bsc.es/[30]; GSE76894,[31]) or by GEO2R (Benjamini & Hochberg; false discovery rate; GSE38642,[32] GSE20966,[33]). For GSE38642,[32] the differential expression of genes in islets was analyzed by stratifying the donors on T2D status or HbA1c (hyperglycemic; HbA1c $\geq$ 6%).[32]

Glucose tolerance test and plasma insulin measurements

Oral glucose tolerance tests (OGTT) were performed on overnight-fasted mice. Blood glucose levels were measured (FreeStyle Optium *Neo* glucometer, Abbott) before (0) and 15, 30, 60, 90, 120 and 150 min after oral glucose administration (1.5 g/kg body weight). Blood samples were collected (tubes containing 300UI Heparin/lithium and 1mg NaF/ml) before (0) and 20 min after glucose administration. Plasma insulin,[41] glucagon, GIP, GLP-1 levels were determined using the Ultra-Sensitive Mouse Insulin, mouse glucagon, mouse total GLP-1 and mouse active GIP ELISA Kits (Crystal Chem).

Mouse islet isolation, cell culture and medium

Islets were isolated after collagenase digestion of the pancreas,[17,41] and were cultured in RPMI-1640 containing 10 mM glucose and 10% (vol./vol.) FCS. Some islets were dispersed in clusters of cells with trypsin and plated on glass coverslips (n = 1.53) in RPMI-1640. The medium was a bicarbonate buffered (KRB) solution containing (mM): NaCl 120, KCl 4.8, CaCl2 2.5, MgCl2 1.2 and NaHCO3 24. It was gassed with O2:CO2 (95:5) to maintain pH 7.4 and supplemented with 1 mg/mL BSA.

Insulin secretion

Mouse islets were preincubated for 20 min in KRB with 8 mM glucose before being distributed in batches of 3 islets for the incubation. Islets were incubated for 1 h at 37°C in 800 μL of KRB supplemented with the indicated concentration of peptides in the presence of 8 mM glucose. Supernatants were collected and islets were harvested in 150 μL acid ethanol for insulin content. Human islets were distributed in batches of 10 and were preincubated in 6 mM glucose at 37°C in 800 μL KRB. After 30 min, supernatant corresponding to basal secretion were collected and islets were stimulated with 6 mM glucose supplemented with the indicated concentration of peptides for 1 h. For insulin secretion from mouse/human islets infected with adenoviruses, due to the 3D structure of islets and the fact that only 2–3 layers of cells are reached by adenoviruses (personal observations, and[81]), only small/medium islets (100 μm–200 μm) were infected with adenoviruses and used for insulin secretion. GFP or ARRB2-GFP was expressed in each islet, but expression was variable from islet to islet (from very bright to less bright). Fluorescence intensity was checked before the experiment, to assess infection efficiency, but all islets were then used randomly, regardless of their fluorescence intensity since they were handpicked using a bright-field stereomicroscope. At the end of all experiments, supernatants were collected and islets were harvested in 150 μL acid ethanol for insulin content. Insulin was measured by Homogeneous Time Resolved Fluorescence (HTRF) (Insulin ultra sensitive kit, PerkinElmer/Cisbio) according to the manufacturer's instructions. HTRF signals were measured using Pherastar FS (BMG Labtech) microplate reader.

Vectors, adenoviruses generation and adenoviral infection

EPAC2B-camps (a gift from V. Nikolaev)[75] was digested with NotI, blunted and further digested with HindIII. The released fragment was ligated into HindIII and EcoRV sites of pShuttle-CMV. pcDNA3-AKAR3 (a gift from J. Zhang)[76] was digested with HindIII and EcoRV and ligated into pShuttle-CMV. EGFP-EPAC2 (a gift from L. Quilliam),[77] was digested with NheI, HpaI and SphI. The released fragment was blunted and ligated into EcoRV sites of pShuttle-CMV. The desired direction for the insert was evaluated using NotI. ARRB2-GFP inserted in pEGFP-N1 (a gift from M Scott)[78] was amplified by PCR using Phusion High fidelity polymerase (NEB) with the following primers ATCTTCTAGAGCTAGCGCCACCATGGGTGAAA and ATCTGATATCATCCTTTACTTGTACAGCTCGTCCAT. The product was digested with XbaI and EcoRV, resolved by agarose gel electrophoresis and ligated into pShuttle-CMV. Recombination with pAdEasy-1, transfection into HEK293 cells (ATCC) and viral amplification were performed as described.[82] The generation of EKAR,[41] D4ER[79] and PKCβII (a kind gift from G.A. Rutter)[80] adenoviruses have been described elsewhere, and were reamplified in house. To downregulate the expression of ARRB2 in human islets, islets were adenovirally transduced using ShRNA-hARRB2 (Ad-mCherry-U6-h-ARRB2-shRNA; #shADV-

201476 from Vector Biolabs) and compared with islets transduced with ShRNA-scramble (Ad-mCherry-U6-scrmb-shRNA; #1781 from Vector Biolabs). The expression of proteins and insulin secretion were assessed 72 h after transduction. Transduction for 48 h was not sufficient to downregulate significantly ARRB2 (not shown), whereas transduction for 96 h decreased ARRB2 expression similarly to 72 h. mCherry fluorescence illustrates only the transfection efficacy and is not correlated to ARRB2 expression, as the ShRNA is expressed under the control of U6 promoter while mCherry was under the control of CMV promoter. As already reported for other probes adenovirally transduced in mouse β-cells,[41] we observed that the encoded proteins were preferentially expressed in β-cells compared to non-β-cells. For instance, of the GFP-EPAC2-positive cells, 92% (68/74 cells) were also positive for insulin, while only 8% (6/74) of glucagon-positive cells showed a very weak expression. Of the EPAC2B-camps positive cells, 97% (71/73) were also positive for insulin, while only 3% (2/73) of glucagon-positive cells showed a very weak expression. Of the ARRB2-GFP positive cells, 94% (64/68) were also positive for insulin, while only 6% (4/68) of glucagon-positive cells showed a very weak expression. None of the cells were positive for somatostatin. Dispersed islet cells were overnight infected with the adenoviruses.

cAMP, PKA, ERK1/2, $[Ca^{2+}]_{ER}$, DAG and $[Ca^{2+}]_c$ measurements

The imaging experiments were performed using an Olympus IX70 microscope equipped with a ×60/1.35 objective, Lambda DG-4 exciter (Sutter Instruments), and an EMCCD camera (Evolve 512, Photometrics) controlled by MetaFluor software (Molecular devices). Briefly, 18 h (cAMP production, PKA and ERK1/2) or 48 h (D4ER) after infection, cells were placed into a temperature-controlled perifusion chamber. cAMP production, PKA and ERK1/2 activities and free Ca^{2+} concentration in the endoplasmic reticulum ($[Ca^{2+}]_{ER}$), were measured using Epac2B-camps[75,83], AKAR3,[76] EKAR[41] and D4ER[79] FRET based sensors, respectively. Dispersed islet cells were excited every 5 s at 436 nm and the emitted fluorescence was filtered at 480 nm for cyan fluorescent protein (CFP) and 540 nm for Yellow Fluorescent Protein (YFP) using a OptoSpin fast spinning (Cairn Research, UK). The results are calculated and reported as ratio (YFP/CFP) using the MetaFluor software. Fluorescence was normalized as indicated in figures. For EPAC2B-camps, an increase in cAMP production is reported as a decrease of FRET, but for clarity reasons the curves are represented inverted (i.e., an increased signal represents an increase in cAMP production). For $[DAG]_c$, Upward DAG[25] (Montana Molecular) was delivered via a BacMam infection, according to the manufacturer's guidelines. Imaging experiments were performed 48 h after infection. Dispersed islet cells were excited every 5 s at 480 nm and the emitted fluorescence was filtered at 535 nm. Fluorescence was normalized to the initial fluorescence and reported as F/F0. For $[Ca^{2+}]_c$, dispersed islet cells were loaded with 2 μM Fura-2 Leakage Resistant-AM (Interchim) for 1 h, placed into a temperature-controlled perifusion chamber and excited every 3 s at 340 and 380 nm; the emitted light was recorded at 510 nm[17,41]. Ca^{2+}-free medium were supplemented with 0.5 mM EGTA.

Total internal refection fluorescence (TIRF) microscopy

A Deltavision OMX-V4 (GE Healthcare Life Sciences) equipped with a ×100 objective lens with 1.49 numerical aperture and EMCCD cameras (Evolve 512B; Photometrics, Tucson, USA) was used. Each probe (GFP-EPAC2,[77] PKCβII-GFP[80]) was excited with a 488 nm laser and emission was filtered at 528/48 nm. Images were collected every 3 s with 10 ms exposure, alternating between three different fields. Experiments were performed in a 37°C temperature-controlled chamber. Fluorescence was normalized to the initial fluorescence and reported as F/F0.

Immunofluorescence

Dispersed mouse islet cells were preincubated for 15 min in 8 mM glucose (G8) before being incubated for 25 min in the presence or absence of GLP-1 or GIP, as indicated. Cells were fixed for 20 min (4% paraformaldehyde; 80 mM NaF for phospho-proteins), overnight incubated with primary antibodies (key resources table) followed by 1 h incubation with secondary antibodies and DAPI (key resources table). For *p*-ERK1/2, a methanol treatment after paraformaldehyde fixation was required.[41] For *p*-FAK and *p*-Paxillin imaging, an insulin staining was also performed and Alexa 680 anti-guinea pig secondary antibody was used. This strategy enabled to identify β-cells. Then the focus was made on the interface/adhesion points where spots of *p*-FAK were visible. Insulin was not imaged because the focal plane used did not ensure an appropriate focus for insulin. All antibodies are commercially available (key resources table) and were validated by companies for immunofluorescence, but also verified in our team before being used. Results were reproducible over time, using different antibody lots. For the F-actin staining, cells were incubated with Alexa Fluor 488 Phalloidin (Cell Signaling Technology) for 15 min after the incubation with secondary antibody for insulin, according to manufacturer's protocol. Experimenters were blinded to group assignment. Cells were imaged using an ×100 objective from AxioImager Apotome microscope (Zeiss) using the ZenBlue software. All of the images from *Arrb2*$^{+/+}$ and *Arrb2*$^{-/-}$ and different conditions (in the presence or absence of GLP-1/GIP) from the same islet preparation were taken the same day to avoid a possible time related fading out of the samples. 50 cells per coverslip/mouse (n = 1) were imaged and saved in ".czi" (rather than "tiff") format allowing to save the entire image parameters and were quantified using ImageJ, as already reported.[41] Each dot represents the average of ~30–50 cells from 1 mouse. Cells were pre-incubated 2 h with the PI3Kγ inhibitor AS604850 (1μM) and 15 min with barbadin (30 μM) prior the experiments. For *p*-FAK/p-Pax images, spots were counted using find single point maxima on a light background after Laplacian filtering using ImageJ.

Real-time quantitative RT-PCR

Total RNAs were extracted and DNase-treated using the RNAeasy microkit (Qiagen) and reverse-transcribed with MoMuLVRT (Life Technology) according to the manufacturers' instructions. To quantify the expression of genes, primer pairs were designed and

validated (Qiagen-Operon, Table S1) for real-time, quantitative PCR, which was performed with Roche LC480 and the Light Cycler 480 SybrGreen Master Mix (Roche).[41] GeNorm[84] was used to select the most appropriate housekeeping genes. The level of expression of each gene X was normalized to the geometric mean of the levels of expression of *ARP* and *L31* according to the formula X/geometric mean (*ARP*; *L31*) = $2^{-(Cp(X)-\text{arithmetic mean }(Cp(ARP);Cp(L31)))}$, where Cp is the crossing point.

Western blotting

Human islets were washed with cold PBS and lysed for 10 min at 4°C in lysis buffer, sonicated for 10 s and centrifuged at 10,000 rpm for 10 min.[68] Proteins (25–50 μg/lane) were separated on a 4–12% Bis-Tris (or 3–8% Tris-Acetate) NuPAGE gel and blotted onto a PVDF membrane (FluoroTrans; VWR). Membranes were probed overnight at 4°C with primary antibodies (Cell Signaling Technology). Horse-radish peroxidase-conjugated secondary antibodies were from Cell signaling. Proteins were visualized by enhanced chemiluminescence (Millipore) on ChemiDoc camera (Bio-Rad) and protein expression levels were quantified using the ImageJ software.

QUANTIFICATION AND STATISTICAL ANALYSIS

Unless otherwise indicated, data are mean ± SEM for the indicated number of observations. Statistical details of experiments can be found in figure legends. GraphPad Prism 9.2.0 software was used. Data normality was assessed using D'Agostino-Person test and/or Shapiro-Wilk test. Statistically significant differences between groups were assessed by Student's two-tailed unpaired or paired *t* test (pairwise comparisons), or by one-way or two-way ANOVA (multiple comparisons). For ANOVA, when the global factor effect was shown significant, post-hoc tests (indicated in figure legends) were performed to get adjusted p values. We used Sidak's post-hoc tests when selected pairs of columns were compared, and Tukey's post-hoc testing for multiple comparisons. A p value less than 0.05 was considered significant.